

Solutions to the Problems

Problems of Chapter 2

2.1 Floating-Car Data

GPS data provide space-time data points and (anonymized) IDs of the equipped vehicles. We can obtain their *trajectories* by connecting the data points in a space-time diagram (via a map-matching process). From the trajectories, we can infer the speed by taking the gradients. Low speeds on a highway or freeway, e.g., 30 km/h, usually indicate a *traffic jam*. Since the data provide spatiotemporal positions of the vehicles, we can deduce the location of congested zones, including their upstream and downstream boundaries, at least, if the penetration rate of equipped vehicles with activated communication is sufficiently high.¹ However, GPS measurements are only accurate to the order of 10 m and careful map-matching/error checking is necessary to exclude, for example, stopped vehicles on the shoulder or at a rest area, or vehicles on a parallel road. Moreover, due to this resolution limit, GPS data do *not* reveal lane information, nor information on *lane changes*. Since the percentage of equipped vehicles with connected devices is low, variable, and unknown, we can *not* deduce extensive quantities (traffic density and flow) from this type of data.

To wrap it up: (1) yes; (2) no; (3) no; (4) no; (5) yes; (6) yes.

2.2 Analysis of Empirical Trajectory Data

1. *Flow, density, and speed*: Using the spatiotemporal region $[10\text{ s}, 30\text{ s}] \times [20\text{ m}, 80\text{ m}]$ suggested for a representative free-flow situation, we obtain by trajectory counting:

¹ On major roads with high traffic flow, 0.5 % of the vehicles are typically enough; on smaller roads, we need a significantly higher percentage.

$$Q_{\text{free}} = \frac{11 \text{ vehicles}}{20 \text{ s}} = 1,980 \text{ vehicles/h}, \quad \rho_{\text{free}} = \frac{3 \text{ vehicles}}{60 \text{ m}} = 60 \text{ vehicles/km}.$$

The speed can be deduced either from the gradient of the trajectories or from the hydrodynamic relation Q/ρ :

$$V_{\text{free}}^{\text{gradient}} = \frac{60 \text{ m}}{5 \text{ s}} = 43.2 \text{ km/h}, \quad V_{\text{free}}^{\text{hyd}} = \frac{Q_{\text{free}}}{\rho_{\text{free}}} = 39.6 \text{ km/h}.$$

This discrepancy is tolerable in view of the reading accuracy (one may also count 12 vehicles in 20 s, yielding $Q = 2,160$ vehicles/h and thus $\rho = 43.2$ km/h). For congested traffic, we use, again, the suggested spatiotemporal region [50 s, 60 s] \times [40 m, 100 m] and obtain analogously

$$Q_{\text{cong}} = \frac{2 \text{ vehicles}}{10 \text{ s}} = 720 \text{ vehicles/h}, \quad \rho_{\text{cong}} = \frac{6 \text{ vehicles}}{60 \text{ m}} = 1,000 \text{ vehicles/km},$$

$$V_{\text{cong}}^{\text{hyd}} = \frac{Q_{\text{cong}}}{\rho_{\text{cong}}} = 7.2 \text{ km/h}.$$

2. Propagation velocity: The stop-and-go wave can be identified by the spatiotemporal region with nearly horizontal trajectories. First, we observe that, in the diagram, the gradient of the (essentially parallel) upstream and downstream wave boundaries are negative, i.e., the wave propagates *against* the direction of traffic. To determine the propagation velocity, we estimate from the diagram

$$c \approx -\frac{140 \text{ m}}{(60 - 33) \text{ s}} = -5.2 \text{ m/s} = -19 \text{ km/h}.$$

3. Travel time increase: Without being obstructed by the traffic wave, the considered vehicle entering at $t = 50$ s into the investigated road section ($x = 0$) would leave the section ($x = L = 200$ m) after about 16 s. This can be deduced either by linearly extrapolating the first seconds of the trajectory, or by the quotient L/V_{free} . The *actual* vehicle leaves the investigated region at $t = 86$ s. Thus, the delay imposed by this traffic wave on the vehicle is 20 s.

4. Lane-changing rate: By counting all lane changes entering and leaving the considered lane in the spatiotemporal region [0 s, 80 s] \times [0 m, 140 m], i.e., trajectories beginning or ending inside this region,² we obtain the lane-changing rate by

$$r \approx \frac{6 \text{ changes}}{80 \text{ s } 140 \text{ m}} = 0.00054 \frac{\text{changes}}{\text{m s}} \approx 1,900 \frac{\text{changes}}{\text{km h}}.$$

² Outside this region, a positive bias is unavoidable because real lane changes cannot be distinguished from the begin/end of recorded trajectories.

2.3 Trajectory Data of “Obstructed” Traffic Flow

1. The trajectory data shows a queue at a traffic light. The horizontal bar marks the position of the traffic light and the duration of the red light phase.
2. Flow $Q_{\text{in}} = 5$ trajectories per $20 \text{ s} = 0.25 \text{ vehicles/s} = 900 \text{ vehicles/h}$.
3. Following the trajectory which starts at $x = -80 \text{ m}$, $t = -16 \text{ s}$ and which ends at $(x, t) = (80 \text{ m}, 0 \text{ s})$, we get the speed

$$v_{\text{in}} = \frac{160 \text{ m}}{16 \text{ s}} = 10 \text{ m/s} = 36 \text{ km/h}.$$

The density is read off the diagram as one trajectory per 40 m or is calculated using $\rho = Q/v$. Either way yields $\rho = 25 \text{ vehicles/km}$.

4. Density in the congested area: 8 horizontal trajectories per $40 \text{ m} \Rightarrow \rho_{\text{jam}} = 200 \text{ vehicles/km}$.
5. Outflow after the red light turns green: The best way is to count the number of lines within a 20 s interval above the blue dots marking the end of the acceleration phase, giving 10 lines per 20 s and thus $Q_{\text{out}} = 0.5 \text{ vehicles/s} = 1800 \text{ vehicles/h}$. The speed is the same as in free traffic (the trajectories are parallel to those further upstream), i.e., $V = 36 \text{ km/h}$. The density is obtained again by counting trajectories (two lines per 40 m) or via the hydrodynamic relation, yielding $\rho = 50 \text{ vehicles/km}$.
6. Propagation velocities of the fronts can be read off the chart as the gradient of the front lines (marked by the dots) or using the continuity equation (cf. Chap. 7):

$$\text{free} \rightarrow \text{congested: } v_g^{\text{up}} = \frac{\Delta Q}{\Delta \rho} = \frac{-900 \text{ vehicles/h}}{175 \text{ vehicles/km}} = -5.17 \text{ km/h},$$

$$\text{congested} \rightarrow \text{free: } v_g^{\text{down}} = \frac{\Delta Q}{\Delta \rho} = \frac{1,800 \text{ vehicles/h}}{-150 \text{ vehicles/km}} = -12 \text{ km/h}.$$

7. Without the red light the vehicle entering at $x = -80 \text{ m}$ and $t = 20 \text{ s}$ would have reached the “end” (upper border) of the diagram ($x = 100 \text{ m}$) at $t_{\text{end}} = 38 \text{ s}$. De facto, it arrives at $x = 100 \text{ m}$ at time $t = 69 \text{ s}$, thus delayed by 31 s .
8. The braking distance is $s_b = 25 \text{ m}$, while the distance covered during the acceleration phase is $s_a = 50 \text{ m}$. Thus

$$b = \frac{v^2}{2s_b} = 2 \text{ m/s}^2, \quad a = \frac{v^2}{2s_a} = 1 \text{ m/s}^2.$$

Alternatively, we can calculate the braking distance using the definition of the acceleration and the duration Δt of the acceleration/deceleration:

$$b = -\frac{\Delta v}{\Delta t} = -\frac{-10 \text{ m/s}}{10 \text{ s}} = 2 \text{ m/s}^2, \quad a = \frac{\Delta v}{\Delta t} = \frac{10 \text{ m/s}}{10 \text{ s}} = 1 \text{ m/s}^2.$$

Problems of Chapter 3

3.1 Data Aggregation at a Cross-Section

1. *Flow and speed:* With an aggregation interval $\Delta t = 30$ s and $n_1 = 6$, $n_2 = 4$ measured vehicles on lanes 1 and 2, respectively, the flow and time mean speed on the two lanes are

$$\begin{aligned} Q_1 &= \frac{n_1}{\Delta t} = 0.2 \text{ vehicles/s} = 720 \text{ vehicles/h}, \\ Q_2 &= \frac{n_2}{\Delta t} = 0.133 \text{ vehicles/s} = 480 \text{ vehicles/h}, \\ V_1 &= \frac{1}{n_1} \sum_{\alpha} v_{1\alpha} = 25.8 \text{ m/s}, \quad V_2 = \frac{1}{n_2} \sum_{\alpha} v_{2\alpha} = 34.0 \text{ m/s}. \end{aligned}$$

2. *Density:* When assuming zero correlations between speeds and time headways, the covariance $\text{Cov}(v_{\alpha}, \Delta t_{\alpha}) = 0$. With Eq. (3.20), this means that calculating the true (spatial) densities by Q/V using the arithmetic (time) mean speed gives no bias:

$$\rho_1 = \frac{Q_1}{V_1} = 7.74 \text{ vehicles/km}, \quad \rho_2 = \frac{Q_2}{V_2} = 3.92 \text{ vehicles/km}.$$

3. *Both lanes combined:* Density and flow are *extensive quantities* increasing with the number of vehicles. Therefore, building the total quantities by simple summation over the lanes makes sense:

$$\rho_{\text{tot}} = \rho_1 + \rho_2 = 11.66 \text{ vehicles/km}, \quad Q_{\text{tot}} = Q_1 + Q_2 = 1,200 \text{ vehicles/h}.$$

Since speed is an *intensive* quantity (it does not increase with the vehicle number), summation over lanes makes no sense. Instead, we define the effective aggregated speed by requiring the hydrodynamic relation to be valid for total flow and total density as well:

$$V = \frac{Q_{\text{tot}}}{\rho_{\text{tot}}} = \frac{\rho_1 V_1 + \rho_2 V_2}{\rho_{\text{tot}}} = \frac{Q_{\text{tot}}}{Q_1/V_1 + Q_2/V_2} = 28.5 \text{ m/s} = 102.9 \text{ km/h}.$$

By its derivation from the hydrodynamic relation, this effective speed is the space mean speed rather than the time mean speed measured directly by the detectors. We notice that the effective speed is simultaneously the *arithmetic mean* weighted with the densities, and the *harmonic mean* weighted with the flows. However, the weighting with the densities requires that the density estimates itself are known without bias. This is the case here but not generally. Since flows can always be estimated without systematic errors from stationary detectors, the harmonic mean weighted with the flows is preferable.

4. *Fraction of trucks*: Two out of six (33 %) are in the right lane, none in the left, two out of ten (20 %) total. Notice again that the given percentages are the fraction of trucks *passing* a fixed location (*time mean*). In the same situation, we expect the fraction of trucks observed by a “snapshot” of a road section at a fixed time (*space mean*). To be higher, at least if trucks are generally slower than cars

3.2 Determining Macroscopic Quantities from Single-Vehicle Data

The distance headway $\Delta x_\alpha = 60$ m is constant on both lanes. All vehicles are of the same length $l = 5$ m and all vehicles on a given lane l (left) or r (right) have the same speed $v_\alpha^l = 144$ km/h = 40 m/s and $v_\alpha^r = 72$ km/h = 20 m/s, respectively.

1. *Time gap / headway*: The headways $\Delta t_\alpha = \Delta x_\alpha / v_\alpha$ are

$$\Delta t_\alpha^l = \frac{60 \text{ m}}{40 \text{ m/s}} = 1.5 \text{ s}, \quad \Delta t_\alpha^r = \frac{60 \text{ m}}{20 \text{ m/s}} = 3.0 \text{ s}.$$

The time gaps T_α are equal to the headway minus the time needed to cover a distance equal to the length of the leading vehicle, $T_\alpha = \Delta t_\alpha - \frac{l_\alpha - 1}{v_{\alpha-1}}$. Since all vehicle lengths are equal, this results in

$$T_\alpha^l = \frac{60 \text{ m} - 5 \text{ m}}{40 \text{ m/s}} = 1.375 \text{ s}, \quad T_\alpha^r = \frac{60 \text{ m} - 5 \text{ m}}{20 \text{ m/s}} = 2.75 \text{ s}.$$

2. *Macroscopic quantities*: We assume an aggregation time interval $\Delta t = 60$ s. However, due to the stationary situation considered here, any other aggregation interval will lead to the same results. Directly from the definitions of flow, occupancy, and time-mean speed, we obtain for each lane

$$\begin{aligned} Q^l &= \frac{1}{\Delta t_\alpha^l} = \frac{1}{1.5 \text{ s}} = 2,400 \text{ vehicles/h}, & Q^r &= \frac{1}{\Delta t_\alpha^r} = \frac{1}{3 \text{ s}} = 1,200 \text{ vehicles/h}. \\ O^l &= \frac{0.125}{1.5} = 0.083 = 8.3 \%, & O^r &= \frac{0.25}{3.0} = 0.083 = 8.3 \%. \\ V^l &= 144 \text{ km/h}, & V^r &= 72 \text{ km/h}. \end{aligned}$$

Due to the homogeneous traffic situation, the arithmetic and harmonic time-mean speed are the same and directly given by the speed of the individual vehicles.

Totals and averages of both lanes: As already discussed in Problem 3.1 summing over the lanes to obtain a total quantity makes only sense for extensive quantities (Q, ρ) but not for the intensive ones (V, O).

Flow:

$$Q_{\text{tot}} = \frac{\Delta N}{\Delta t} = \frac{\Delta N^l + \Delta N^r}{\Delta t} = 3,600 \text{ vehicles/h}, \quad Q = \frac{Q_{\text{tot}}}{2} = 1,800 \text{ vehicles/h}.$$

Occupancy:

$$O = O^l = O^r = 0.083.$$

Arithmetic time mean speed:

$$V = \frac{1}{\Delta N} \sum_{\alpha} v_{\alpha} = \frac{40 \cdot 40 \text{ m/s} + 20 \cdot 20 \text{ m/s}}{60} = 120 \text{ km/h}.$$

Harmonic time mean speed:

$$V_H = \frac{\Delta N}{\sum 1/v_{\alpha}} = \frac{60}{\frac{40}{40 \text{ m/s}} + \frac{20}{20 \text{ m/s}}} = 108 \text{ km/h}.$$

We observe that the arithmetic mean is larger than the harmonic mean.

Which mean? In traffic flow, there are four sensible ways to average, consisting of the four combinations of (i) one of two physical ways (time mean and space mean), (ii) one of two mathematical ways (arithmetic and harmonic).

- *Time mean* means averaging at a fixed location over some time interval as done by stationary detectors.
- *Space mean* means averaging at a fixed time over some space interval (road section), e.g., when making a snapshot of the traffic flow.

For the *space mean*, we have (cf. the previous problem)

$$V = \frac{\rho_1 V_1 + \rho_2 V_2}{\rho_{\text{tot}}} = \frac{Q_{\text{tot}}}{Q_1/V_1 + Q_2/V_2}$$

while, for the time mean, we simply have

$$V = \frac{Q_1 V_1 + Q_2 V_2}{Q_{\text{tot}}}.$$

The time mean is generally larger than the space mean because, at the same partial densities, the class of faster vehicles passes the cross-section more often within the aggregation interval than the vehicles of the slower class do. The arithmetic average is generally larger than the harmonic average which can be shown for any data. Only for the trivial case of identical data, both averages agree.

Here, $\rho_1 = \rho_2$ but $Q_1 \neq Q_2$, so the simple (not weighted) arithmetic average over lanes applies for the space mean speed.

3. *Speed variance between lanes*: Because of identical speeds on either lane, the total variance of the speeds in the left and right lane is the same as the inter-lane variance sought after:

$$\begin{aligned}\sigma_V^2 &= \left\langle (v_\alpha - \langle v_\alpha \rangle)^2 \right\rangle \\ &= \frac{1}{60} \left(40[40 - 33.3]^2 + 20[20 - 33.3]^2 \right) \\ &= 88.9 \text{ m}^2/\text{s}^2.\end{aligned}$$

4. *Total speed variance*: We divide the speed variance

$$\sigma_V^2 = \frac{1}{N} \sum_{\alpha} (v_{\alpha} - V)^2$$

into two sums over the left and right lane, respectively:

$$\sigma_V^2 = \frac{1}{N} \left[\sum_{\alpha_1=1}^{N_1} (v_{\alpha_1} - V)^2 + \sum_{\alpha_2=1}^{N_2} (v_{\alpha_2} - V)^2 \right].$$

Now we expand the two squares:

$$(v_{\alpha_1} - V)^2 = (v_{\alpha_1} - V_1 + V_1 - V)^2 = (v_{\alpha_1} - V_1)^2 + 2(v_{\alpha_1} - V_1)(V_1 - V) + (V_1 - V)^2,$$

where V_1 is the average over lane 1. We proceed analogously for $(v_{\alpha_2} - V)^2$. Inserting this into the expression for σ_V^2 and recognizing that

$$\sum_{\alpha_1} (v_{\alpha_1} - V_1)(V_1 - V) = 0, \quad \sum_{\alpha_2} (v_{\alpha_2} - V_2)(V_2 - V) = 0$$

and

$$\sigma_{V_1}^2 = \frac{1}{N_1} \sum_{\alpha_1=1}^{N_1} (v_{\alpha_1} - V_1)^2$$

and similarly for $\sigma_{V_2}^2$, we obtain

$$\sigma_V^2 = \frac{N_1}{N} \left[\sigma_{V_1}^2 + (V_1 - V)^2 \right] + \frac{N_2}{N} \left[\sigma_{V_2}^2 + (V_2 - V)^2 \right].$$

With $p_1 = N_1/N$ and $p_2 = N_2/N = 1 - p_1$, we get the formula of the problem statement. If $p_1 = p_2 = 1/2$ we have $V = (V_1 + V_2)/2$ and thus

$$\sigma_V^2 = \frac{1}{2} \left[\sigma_{V_1}^2 + \sigma_{V_2}^2 \right] + \frac{(V_1 - V_2)^2}{4}.$$

Notice that this mathematical relation can be applied to both space mean and time mean averages.

Problems of Chapter 4

4.1 Analytical Fundamental Diagram

We have to distinguish between free and congested traffic.

Free traffic:

$$V^{\text{free}}(\rho) = V_0 = \text{const.}$$

Flow by using the hydrodynamic relation:

$$Q^{\text{free}}(\rho) = \rho V^{\text{free}}(\rho) = \rho V_0.$$

Congested traffic: The speed-dependent equilibrium gap between vehicles, $s(v) = s_0 + vT$, leads to the gap-dependent equilibrium speed $V^{\text{cong}}(s)$:

$$V^{\text{cong}}(s) = \frac{s - s_0}{T}.$$

Using the definition of the density ρ , we replace the gap s :

$$\begin{aligned} \rho &= \frac{\text{number of vehicles}}{\text{road length}} \\ &= \frac{\text{one vehicle}}{\text{one distance headway (front-to-front distance)}} \\ &= \frac{1}{\text{vehicle length} + \text{gap (bumper-to-bumper distance)}} = \frac{1}{l + s}. \end{aligned}$$

Thus $s(\rho) = \frac{1}{\rho} - l$ and therefore

$$V^{\text{cong}}(\rho) = \frac{s - s_0}{T} = \frac{1}{T} \left[\frac{1}{\rho} - (l + s_0) \right].$$

The flow-density relation is obtained again by the hydrodynamic relation:

$$Q^{\text{cong}}(\rho) = \rho V^{\text{cong}}(\rho) = \frac{1}{T} [1 - \rho(l + s_0)].$$

The sum $l_{\text{eff}} = l + s_0$ of vehicle length and minimum gap can be interpreted as an *effective* vehicle length (typically 7 m in city traffic, somewhat more on highways). Accordingly, the maximum density is

$$\rho_{\max} = \frac{1}{l + s_0} = \frac{1}{l_{\text{eff}}}.$$

To obtain the critical density ρ_C separating free and congested traffic, we determine the point where the free and congested branches of the fundamental diagram intersect:

$$Q^{\text{cong}}(\rho) = Q^{\text{free}}(\rho) \Rightarrow \rho V_0 T = 1 - \rho(l + s_0) \Rightarrow \rho_C = \frac{1}{V_0 T + l_{\text{eff}}}.$$

This is the “tip” of the triangular fundamental diagram, and the corresponding flow is the capacity C (the maximum possible flow):

$$C = Q^{\text{cong}}(\rho_C) = Q^{\text{free}}(\rho_C) = \frac{1}{T} \left(\frac{1}{1 + \frac{l_{\text{eff}}}{V_0 T}} \right). \quad (2.1)$$

The capacity C is of the order of (yet always less than) the inverse time gap T . The lower the free speed V_0 , the more pronounced the discrepancy between the “ideal” capacity $1/T$ and the actual value.

Given the numeric values stated in the problem, we obtain the following values for ρ_{\max} , ρ_C , and C :

$$\begin{aligned} \rho_{\max} &= 143 \text{ vehicles/km}, & \rho_C &= 16.6 \text{ vehicles/km}, \\ C &= 0.552 \text{ vehicles/s} = 1,990 \text{ vehicles/h}. \end{aligned}$$

4.2 Flow-Density Diagram of Empirical Data

The free velocity can be read off the speed-density diagram (at low densities):

$$V_{A8}^{\text{free}} = 125 \text{ km/h}, \quad V_{A9}^{\text{free}} = 110 \text{ km/h}.$$

(Dutch police is very rigorous in enforcing speed limits and uses automated systems to do so. This explains why few people drive faster than 110 km/h.)

The flow-density diagram immediately shows the maximum density (the density where the flow data drop to zero at the right-hand side) and the capacity (maximum flow):

$$\begin{aligned} \rho_{A8}^{\max} &= 80 \text{ vehicles/km}, & \rho_{A9}^{\max} &= 110 \text{ vehicles/km}, \\ C_{A8} &= 1,700 \text{ vehicles/h}, & C_{A9} &= 2,400 \text{ vehicles/h}. \end{aligned}$$

The headways can be calculated by solving the capacity equation (2.1) for T ,

$$T = \frac{1 - \frac{l_{\text{eff}}C}{V_0}}{C} = \frac{1 - \frac{C}{V_0\rho_{\text{max}}}}{C},$$

and thus

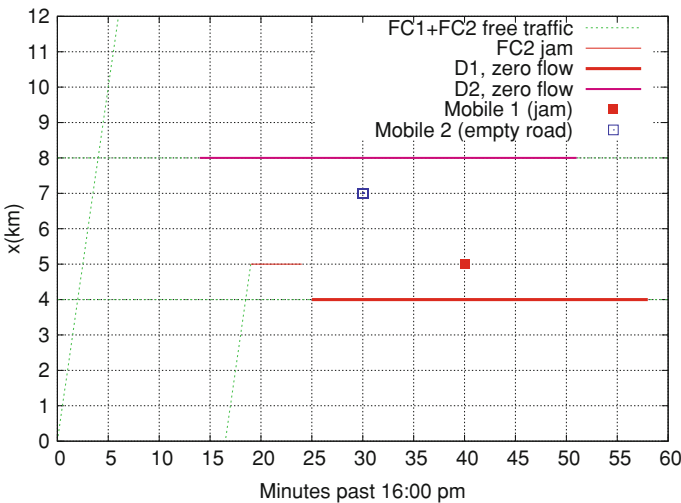
$$T_{A8} = 1.91 \text{ s}, \quad T_{A9} = 1.27 \text{ s}.$$

One cautionary note is in order: If the data of the scatter plots are derived from arithmetic time mean speeds via the relation $\rho = Q/V$ (as it is the case here), the density of congested traffic flow, and in the consequence T , will be underestimated. To a lesser extent, this also applies to harmonic averages (cf. Fig. 4.10). In the Sects. 8.5.3 and 16.3, we will learn about more robust estimation methods based on propagation velocities.

Problems of Chapter 5

5.1 Reconstruction of the Traffic Situation Around an Accident

Part 1: In the space-time diagram below, thin dashed green lines mark confirmed free traffic while all other information is visualized using thicker lines and different colors. The respective information is denoted in the key. The signal “zero flow” means “I do not know; either empty road or stopped traffic”.



Part 2: The information of the first floating car (FC1) tells us the speed in free traffic, $V_{\text{free}} = 10 \text{ km}/5\text{min} = 120 \text{ km/h}$. From the second floating car (FC2) we know that an upstream jam front passes $x = 5 \text{ km}$ at 4:19 pm.

The stationary detectors D1 at $x = 4 \text{ km}$ and D2 at 8 km both report zero flows in a certain time interval but this does not tell apart whether the road is maximally congested or empty. However, we additionally know by the two mobile phone calls that the road is fully congested at 5 km while it is empty at 7 km . The congestion at 5 km is also consistent with the trajectory of the second floating car. Since downstream jam fronts (transition jam \rightarrow free traffic) are either stationary or propagate upstream at velocity $c \approx -15 \text{ km/h}$ but never downstream (apart from the special case of a moving bottleneck), we know that the missing vehicle counts of D1 are the consequence of standing traffic while that of D2 reflect an empty road (at least when ignoring the possibility that there might be another obstruction more downstream causing a second jam).

With this information, we can estimate the motion of the upstream jam front. Assuming a constant propagation velocity c^{up} , we determine this velocity from the spatiotemporal points where detector D1 and the second floating car encounter congestion, respectively:

$$c^{\text{up}} = \frac{-1 \text{ km}}{6 \text{ min}} = -10 \text{ km/h}.$$

The motion of this front is another strong evidence that D2 does not measure a transition from free to fully congested traffic but from free traffic to no traffic at all at $x = 8 \text{ km}$ and $t = 4:14 \text{ pm}$: Otherwise, the propagation velocity c^{up} would be $-4 \text{ km}/5 \text{ min} = -48 \text{ km/h}$ in this region which is not possible even if we do not require c^{up} to be constant: The largest possible negative velocity c^{up} , realized under conditions of maximum inflow against a full road block, is only insignificantly larger in magnitude than $|c^{\text{down}}| \approx 15 \text{ km/h}$.

Now we have enough information to determine location and time of the initial road block (accident). Intersecting the line

$$x^{\text{up}}(t) = 4 \text{ km} + c^{\text{up}}t - 25 \text{ min} = 4 \text{ km} - \frac{t - 25 \text{ min}}{6} \text{ km/min}$$

characterizing the upstream front with the trajectory $x_{\text{last}}(t)$ of the last vehicle that made it past the accident location,

$$x_{\text{last}}(t) = 8 \text{ km} + v_0(t - 14 \text{ min}) = 8 \text{ km} + (t - 14 \text{ min}) 2 \text{ km/min}$$

yields location and time of the road block:

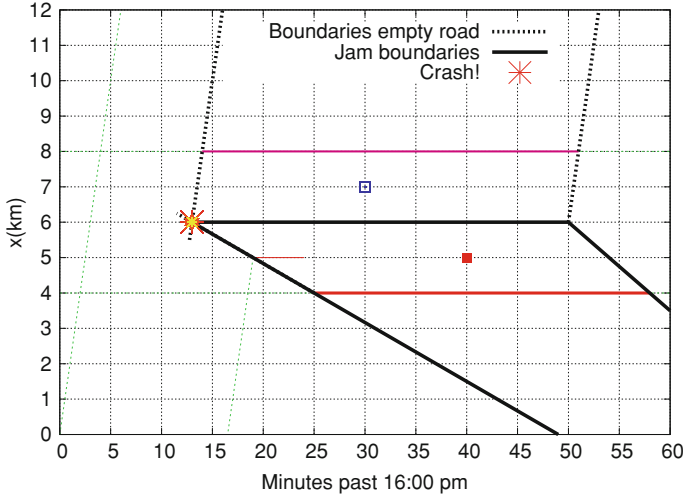
$$x_{\text{crash}} = 6 \text{ km}, \quad t_{\text{crash}} = 4:13 \text{ pm}.$$

Part 3: After the accident site is cleared, the initially stationary downstream jam front (fixed at the accident site) starts moving at the characteristic velocity $c^{\text{down}} =$

$-15 \text{ km/h} = -1 \text{ km}/4 \text{ min}$. Since the detector at $x = 4 \text{ km}$ (D1) detects non-zero traffic flow from 4:58 pm onwards, the front is described by

$$x^{\text{down}}(t) = 4 \text{ km} + c^{\text{down}}(t - 58 \text{ min}).$$

Obviously, the accident location ($x_{\text{crash}} = 6 \text{ km}$) is cleared exactly at the time where the moving downstream jam front crosses the accident site (cf. the figure), i.e., at $t_{\text{clear}} = 4:50 \text{ pm}$.



5.2 Dealing with Inconsistent Information

Using equal weights, $V = \frac{1}{2}(V_1 + V_2)$, the error variance is

$$\sigma_V^2 = \frac{1}{4} (\sigma_1^2 + \sigma_2^2) = \frac{1}{4} (\sigma_1^2 + 4\sigma_1^2) = \frac{5}{4}\sigma_1^2,$$

assuming negligible systematic errors and independent random errors. Consequently, the error increases by a factor of $\sqrt{5/4}$ due to the inclusion of the noisy floating-car data. Using optimal weights,

$$V_{\text{opt}} = \frac{1}{5}(4V_1 + V_2),$$

yields the error variance

$$(\sigma_V^2)_{\text{opt}} = \frac{1}{25} (16\sigma_1^2 + \sigma_2^2) = \frac{1}{25} (16\sigma_1^2 + 4\sigma_1^2) = \frac{4}{5}\sigma_1^2.$$

This means, adding floating-car data with a small weight to the stationary detector data *reduces* the uncertainty by a factor of down to $\sqrt{4/5}$, in spite of the fourfold variance of the floating-car data compared to the stationary detector data.

Problems of Chapter 6

6.1 Speed Limit on the German Autobahn?

The *safety aspect* of speed limits cannot be modeled or simulated by traffic-flow models simply because these models are calibrated to normal situations (including traffic jams). However, accidents are typically the consequence of a series of unfortunate circumstances and extraordinary driving behavior which is not included in the models. In contrast, the effect on *fuel consumption* can be modeled and simulated reliably by combining microscopic or macroscopic traffic flow models with the corresponding models for fuel consumption or emissions, cf. Chap. 20. To assess the *economic effect* of speed limits, including social welfare or changed traffic patterns, one needs models for traffic demand and route choice, i.e., models of the domain of transportation planning. Traffic flow models are suited, however, to investigate certain environmental and societal aspects on a smaller scale. For example, traffic flow models in connection with consumption/emission models describe the direct effect of speed limits on emissions. Furthermore, since speed limits change the propensity for traffic breakdowns and traffic flow/emission models can describe this influence as well as the changed emissions in the jammed state, these models also describe the indirect effect via traffic breakdowns.

Problems of Chapter 7

7.1 Flow-Density-Speed Relations

We require

$$Q_{\text{tot}} = \sum_i Q_i = \sum_i \rho_i V_i = \rho_{\text{tot}} V$$

which we can fulfil by suitably defining the effective average V of the local speed across all lanes. Solving this condition for V directly gives

$$V = \sum_i \frac{\rho_i}{\rho_{\text{tot}}} V_i = \sum_i w_i V_i,$$

i.e., the definition (7.6) of the main text.

7.2 Conservation of Vehicles

In a closed ring road, the vehicle number $n(t)$ is the integral of the total vehicle density $\rho_{\text{tot}} = I(x)\rho$ over the complete circumference of the ring. Applying Eq. (7.15) for $v_{\text{rmp}} = 0$ and the hydrodynamic relation $\rho V = Q$, we obtain for the rate of change of the vehicle number

$$\frac{dn}{dt} = - \oint \left(I(x) \frac{\partial Q(x, t)}{\partial x} + Q(x, t) \frac{dI}{dx} \right) dx = - \oint \frac{\partial (I(x) Q(x, t))}{\partial x} dx = I Q|_{x_a}^{x_e}.$$

If the road is closed, we have $x_e = x_a$, so $\frac{dn}{dt} = 0$ and the total vehicle number n does not change over time.

7.3 Continuity Equation I

(i) The continuity equation for $x < 0$ or $x > L = 300$ m, i.e., outside of the merging region, has no source terms and reads

$$\frac{\partial \rho}{\partial t} + \frac{\partial Q}{\partial x} = 0.$$

In the merging region $0 \leq x \leq L$, we have an additional source term $v_{\text{rmp}}(x, t)$ that generally depends on space and time:

$$\frac{\partial \rho}{\partial t} + \frac{\partial Q}{\partial x} = v_{\text{rmp}}(x, t).$$

Now we assume that v_{rmp} is constant with respect to x over the merging region L . In view of the definition of v , this means that the differential merging rate on a small segment of the merging lane, divided by the number of main-road lanes, is constant. We obtain the connection between the ramp flow Q_{rmp} and v_{rmp} by integrating v over the merging region and requiring that the result is equal to the ramp flow (if there are several ramp lanes, the total ramp flow) divided by the number I of main-road lanes. Thus,

$$\frac{Q_{\text{rmp}}}{I} = \int_0^L v_{\text{rmp}} dx = v_{\text{rmp}} \int_0^L dx = v_{\text{rmp}} L,$$

so

$$v_{\text{rmp}} = \frac{Q_{\text{rmp}}}{IL} = \frac{1}{2} \frac{600 \text{ vehicles/h}}{300 \text{ m}} = 1 \text{ vehicle/m/hour}.$$

(ii) It is easy to generalize the source term $v_{\text{rmp}}(x)$ to inhomogeneous differential merging rates. In the most general case, we prescribe a distribution function of the merging points³ over the length of the merging lane by its probability density $f(x)$:

³ Later on, when we explicitly model lane changes by microscopic models, we will assume instantaneous lane changes, so the merging point is well-defined. For real continuous changes, one can

$$v_{\text{rmp}}(x, t) = \frac{Q_{\text{rmp}}(t)}{I} f(x).$$

For case (i) (constant differential changing rates),

$$f_{\text{uniform}}(x) = \begin{cases} 1/L & \text{if } 0 \leq x \leq L, \\ 0 & \text{otherwise,} \end{cases}$$

i.e., the merging points are uniformly distributed over the interval $[0, L]$. To model drivers who, in their majority, merge in the first half of the length of the merging lane, we prescribe a distribution $f(x)$ which takes on higher values at the beginning than near the end of the lane, e.g., the triangular distribution

$$f_{\text{early}}(x) = \begin{cases} \frac{2(L-x)}{L^2} & \text{if } 0 \leq x \leq L, \\ 0 & \text{otherwise.} \end{cases}$$

If we want to describe a behavior where drivers change to the main road near the end (which applies for some situations of congested traffic, we mirror $f_{\text{early}}(x)$ at $x = L/2$ to arrive at

$$f_{\text{late}}(x) = \begin{cases} \frac{2x}{L^2} & \text{if } 0 \leq x \leq L, \\ 0 & \text{otherwise.} \end{cases}$$

Remark A temporal dependency is modeled directly by a time-dependent ramp flow $Q_{\text{rmp}}(t)$.

7.4 Continuity Equation II

A stationary traffic flow is characterized by zero partial time derivatives, particularly,

$$\frac{\partial \rho(x, t)}{\partial t} = 0, \quad \frac{\partial Q(x, t)}{\partial t} = 0.$$

This simplifies the continuity equation (7.15) for the effective (lane-averaged) flow and density for the most general case including ramps and variable lane numbers to

$$\frac{dQ}{dx} = -\frac{Q(x)}{I(x)} \frac{dI}{dx} + v_{\text{rmp}}(x). \quad (2.2)$$

By the condition of stationarity, the partial differential equation (7.15) for $\rho(x, t)$ and $Q(x, t)$ with the independent variables x and t changes to an ordinary differential

define x to be the first location where a vehicle crosses the road marks separating the on-ramp from the adjacent main-road lane.

equation (ODE) for Q as a function of x . Stationarity also implies that the traffic inflow at the upstream boundary is constant, $Q(x = 0, t) = Q_0$.

(i) We can solve the ODE (2.2) for $v_{\text{rmp}} = 0$ by the standard method of *separating the variables*:

$$\frac{dQ}{Q} = -\frac{dI}{I} \frac{dx}{dx} = -\frac{dI}{I}.$$

Indefinite integration of both sides with respect to the corresponding variable yields $\ln Q = -\ln I + \tilde{C}$ with the integration constant \tilde{C} . Applying the exponentiation on both sides results in

$$Q(x) = \frac{C}{I(x)}$$

where $C = \exp(\tilde{C})$. The new integration constant is fixed by the spatial initial conditions $C = I(x = 0)Q(x = 0) = I_0 Q_0$ where I_0 is the number of lanes at $x = 0$. This also determines the spatial dependency of the flow:

$$Q(x) = \frac{I_0 Q_0}{I(x)}. \quad (2.3)$$

Notice that this is consistent with the stationarity condition $Q_{\text{tot}} = I(x)Q(x) = I_0 Q_0 = \text{const.}$

(ii) To describe an on-ramp or off-ramp merging to or diverging from a main-road with I lanes with a constant differential rate, we set

$$v_{\text{rmp}} = \frac{Q_{\text{rmp}}}{IL} = \text{const.},$$

where $Q_{\text{rmp}} < 0$ for off-ramps. Applying the condition of stationarity to the continuity equation (7.15) assuming a constant number I of lanes results in the ODE

$$\frac{dQ}{dx} = \begin{cases} v_{\text{rmp}} & \text{parallel to merging/diverging lanes,} \\ 0 & \text{otherwise,} \end{cases}$$

with prescribed and constant $Q(x = 0) = Q_0 = Q_{\text{tot}}/I$ at the upstream boundary. In our problem with an off-ramp upstream of an on-ramp (which is the normal configuration at an interchange), we have

$$\frac{dQ}{dx} = \begin{cases} -Q_{\text{off}}/(IL_{\text{off}}) & \text{if } 300 \text{ m} \leq x < 500 \text{ m,} \\ Q_{\text{on}}/(IL_{\text{on}}) & \text{if } 700 \text{ m} \leq x < 1000 \text{ m,} \\ 0 & \text{otherwise.} \end{cases}$$

where $L_{\text{off}} = 200 \text{ m}$, and $L_{\text{on}} = 300 \text{ m}$. We calculate the solution to this ODE by simple integration:

$$Q(x) = \begin{cases} Q_0 & \text{if } x < 300 \text{ m,} \\ Q_0 - Q_{\text{off}}(x - 300 \text{ m})/(IL_{\text{off}}) & \text{if } 300 \text{ m} \leq x < 500 \text{ m,} \\ Q_0 - Q_{\text{off}}/I & \text{if } 500 \text{ m} \leq x < 700 \text{ m,} \\ Q_0 - Q_{\text{off}}/I + Q_{\text{on}}(x - 700 \text{ m})/(IL_{\text{on}}) & \text{if } 700 \text{ m} \leq x < 1,000 \text{ m,} \\ Q_0 + (Q_{\text{on}} - Q_{\text{off}})/I & \text{if } x \geq 1,000 \text{ m.} \end{cases}$$

7.5 Continuity Equation III

The highway initially has $I_0 = 3$ lanes, and a lane drop to 2 lanes over the effective length L :

$$I(x) = \begin{cases} 3 & x < 0, \\ (3 - \frac{x}{L}) & 0 \leq x \leq L, \\ 2 & x > L. \end{cases}$$

Since the traffic demand (inflow) is constant, $Q_{\text{in}} = Q_{\text{tot}}(0) = 3,600$ vehicles/h, and there is no other explicit time dependence in the system, the traffic flow equilibrates to the stationary situation characterized by $\frac{\partial}{\partial t} = 0$:

$$\frac{dQ}{dx} = -\frac{Q(x)}{I(x)} \frac{dI}{dx}.$$

1. The solution for the section with a variable lane number reads [cf. Eq. (2.3)]:

$$Q(x) = \frac{I_0 Q_0}{I(x)} = \frac{Q_{\text{tot}}}{I(x)}.$$

Upstream and downstream of the lane drop, we have $I(x) = \text{const.}$, i.e.,

$$Q(x) = \frac{Q_{\text{tot}}}{I}.$$

In summary, this results in

$$Q(x) = \begin{cases} Q_{\text{tot}}/3 & x < 0, \\ \frac{Q_{\text{tot}}}{3 - \frac{x}{L}}, & 0 \leq x \leq L \\ Q_{\text{tot}}/2 & x > L. \end{cases}$$

Furthermore, the hydrodynamic relation $Q = \rho V$ with $V = 108$ km/h gives the density

$$\rho(x) = \frac{Q}{V} = \begin{cases} 11.11 \text{ /km} & x < 0, \\ \frac{33.33}{3 - \frac{x}{L}} \frac{1}{\text{km}} & 0 \leq x \leq L, \\ 16.67 \text{ /km} & x > L. \end{cases}$$

2. We insert the relation $I(x) = 3 - x/L$ and $dI/dx = -1/L$ for the lane drop and $Q(x) = Q_{\text{tot}}/(3 - x/L)$ for the flow into the right-hand side of Eq. (2.2):

$$\frac{dQ}{dx} = -\frac{Q_{\text{tot}}}{I^2(x)} \frac{\partial I}{\partial x} = \frac{Q_{\text{tot}}}{L \left(3 - \frac{x}{L}\right)^2}.$$

The right-hand side can be identified with the searched-for effective ramp term:

$$v_{\text{rmp}}^{\text{eff}} = \frac{Q_{\text{tot}}}{L \left(3 - \frac{x}{L}\right)^2}.$$

We determine the effective ramp flow corresponding to $v_{\text{rmp}}^{\text{eff}}(x)$ from the point of view of the two remaining through lanes:

$$\begin{aligned} Q_{\text{rmp}}^{\text{eff}} &= 2 \int_0^L v_{\text{rmp}}^{\text{eff}} dx = \frac{2Q_{\text{tot}}}{L} \int_0^L \frac{dx}{\left(3 - \frac{x}{L}\right)^2} = \frac{2Q_{\text{tot}}}{L} \left(\frac{1}{3 - \frac{x}{L}} \right) \Big|_0^L \\ &= \frac{Q_{\text{tot}}}{3} = 1,200 \text{ vehicles/h/lane.} \end{aligned}$$

Here, we used the indefinite integral

$$\int \frac{dx}{\left(3 - \frac{x}{L}\right)^2} = \frac{L}{3 - \frac{x}{L}}.$$

7.6 Continuity Equation for Coupled Maps

Assuming the steady-state condition, $\rho_k(t + \Delta t) = \rho_k(t)$ for all road cells k , we obtain from Eq. (7.16)

$$\begin{aligned} 0 &= Q_k^{\text{up}} \left(1 + \frac{I_{\text{up}} - I_{\text{down}}}{I_{\text{down}}} \right) - Q_k^{\text{down}} + \frac{Q_{k,\text{rmp}}}{I_{\text{down}}} \\ &= Q_k^{\text{up}} \frac{I_{\text{up}}}{I_{\text{down}}} - Q_k^{\text{down}} + \frac{Q_{k,\text{rmp}}}{I_{\text{down}}} \end{aligned}$$

and, after multiplying with I_{down} ,

$$0 = Q_k^{\text{up}} I_{\text{up}} - Q_k^{\text{down}} I_{\text{down}} + Q_{k,\text{rmp}}$$

which is the flow balance given in the problem statement. This balance means that, in steady-state conditions, the ramp flow is equal to the total outflow $Q_k^{\text{down}} I_{\text{down}}$ from a cell minus the total inflow $Q_k^{\text{up}} I_{\text{up}}$ which is consistent with vehicle conservation.

7.7 Parabolic Fundamental Diagram

For the fundamental diagram

$$Q(\rho) = \rho V(\rho) = \rho V_0 \left(1 - \frac{\rho}{\rho_{\max}} \right),$$

the maximum flow (capacity per lane) Q_{\max} is at a density ρ_C . We determine ρ_C , as usual, by setting the gradient $Q'(\rho)$ equal to zero:

$$Q'(\rho_C) = V_0 - 2 \frac{V_0 \rho_C}{\rho_{\max}} = 0 \quad \Rightarrow \quad \rho_C = \frac{1}{2} \rho_{\max}.$$

Hence

$$Q_{\max} = Q(\rho_C) = \frac{\rho_{\max} V_0}{4}.$$

Problems of Chapter 8

8.1 Propagation Velocity of a Shock Wave Free \rightarrow Congested

The triangular fundamental diagram is semi-concave, i.e., the second derivative $Q_e''(\rho)$ is non-positive, and the first derivative $Q_e'(\rho)$ is monotonously decreasing. This means, any straight line connecting two points on the fundamental diagram always lies below or, at most, on the fundamental diagram $Q_e(\rho)$. Consequently, the slope $c_{12} = (Q_2 - Q_1)/(\rho_2 - \rho_1)$ of this line cannot be greater than $Q'(0) = V_0$ and not less than $Q'(\rho_{\max}) = c$ proving the statement. Since this argumentation only relies on the semi-concavity of the fundamental diagram, it can also be applied to the parabolic fundamental diagram of Problem 7.7 leading to $c_{12} \in [-V_0, V_0]$.

8.2 Driver Interactions in Free Traffic

There are not any in this model. If there were interactions, the followers would react to the leaders, so the information of the shock wave would propagate at a lower velocity than the vehicle speed, contrary to the fact.

8.3 Dissolving Queues at a Traffic Light

When the traffic light turns green, the traffic flow passes the traffic light in the maximum-flow state. For the triangular fundamental diagram, the speed at the maximum-flow state is equal to the desired speed and the transition from the waiting

queue (density ρ_{\max}) to the maximum-flow state propagates backwards at a velocity $c = -l_{\text{eff}}/T$ corresponding to the congested slope of the fundamental diagram. In the microscopic picture, every follower starts a time interval T later than its leader and instantaneously accelerates to V_0 (Fig. 8.12). This suggests to interpret T as the reaction time of each driver, so $|c|$ is simply the distance between two queued vehicles divided by the reaction time.

We emphasize, however, that the LWR model does not contain any reaction time. Moreover, the above microscopic interpretation no longer holds for LWR models with other fundamental diagrams. Therefore, another interpretation is more to the point. As above, the driver instantaneously starts from zero to V_0 which follows directly from the sharp macroscopic shock fronts. However, the drivers only start their “rocket-like” acceleration when there is enough time headway at V_0 . Thus, $|c|$ is the distance between two queued vehicles divided by the desired time gap T in car-following mode. Similar considerations apply for concave fundamental diagrams (such as the parabola-shaped of Problem 7.7). This allows following general conclusion:

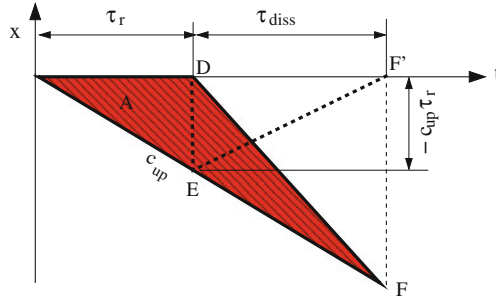
The fact that not all drivers start simultaneously at traffic lights is not caused by reaction times but by the higher space requirement of moving with respect to standing vehicles: It simply takes some time for the already started vehicles to make this space.

8.4 Total Waiting Time During One Red Phase of a Traffic Light

The total waiting time in the queue is equal to the number $n(t)$ of vehicles waiting at a given time, integrated over the duration of the queue: Defining $t = 0$ as the begin of the red phase and $x = 0$ as the position of the stopping line, this means

$$\tau_{\text{tot}} = \int_0^{\tau_r + \tau_{\text{diss}}} n(t) dt = \int_0^{\tau_r + \tau_{\text{diss}}} \int_{x_u(t)}^{x_o(t)} \rho_{\max} dx dt = \rho_{\max} A,$$

i.e., the total waiting time is equal to the jam density times the area of the queue in space-time (cf. the following diagram).



The area of the congested area is equal to the sum of the area of the two right-angled triangles with the legs $(\tau_r, -c_{up}\tau_r)$ and $(\tau_{diss}, -c_{up}\tau_r)$, respectively:

$$\tau_{tot} = \frac{1}{2} \rho_{max} \left(-c_{up} \tau_r^2 - c_{up} \tau_r \tau_{diss} \right).$$

To obtain the second right-angled triangle DEF', we have shifted the point F of the original triangle DEF to F' which does not change the enclosed area. Furthermore, we have the geometrical relation (cf. the figure above)

$$c_{up} \tau_r = (c_{cong} - c_{up}) \tau_{diss},$$

i.e., $\tau_{diss} = c_{up} \tau_r / (c_{cong} - c_{up})$. Inserting this into the expression for τ_{tot} finally gives

$$\tau_{tot} = \frac{1}{2} \rho_{max} \tau_r^2 \frac{c_{up} c_{cong}}{c_{up} - c_{cong}}$$

with

$$c_{up} = \frac{Q_{in}}{Q_{in}/V_0 - \rho_{max}}, \quad c_{cong} = -\frac{1}{\rho_{max} T}.$$

The total waiting time increases with the *square* of the red time.

8.5 Jam Propagation on a Highway I: Accident

Subproblem 1: With the values given in the problem statement, the capacity per lane reads

$$Q_{max} = \frac{V_0}{V_0 T + l_{eff}} = 2,016 \text{ vehicles/h.}$$

The total capacity of the road in the considered driving direction without accident is just twice that value:

$$C = 2Q_{max} = 4,032 \text{ vehicles/h.}$$

This exceeds the traffic demand 3,024 vehicles/h at the inflow ($x = 0$), so no jam forms before the accident, and only road section 1 exists. Since there are neither changes in the demand nor road-related changes, traffic flow is stationary and the flow per lane is constant:

$$Q_1 = \frac{Q_{\text{in}}}{2} = 1,512 \text{ vehicles/h}, \quad V_1 = V_0 = 28 \text{ m/s}, \quad \rho_1 = \frac{Q_1}{V_0} = 15 \text{ vehicles/km}.$$

This also gives the travel time to traverse the $L = 10 \text{ km}$ long section:

$$t_{\text{trav}} = \frac{L}{V_0} = 357 \text{ s}.$$

Subproblem 2: At the location of the accident, only one lane is open, so the bottleneck capacity

$$C_{\text{bottl}} = Q_{\text{max}} = 2,016 \text{ vehicles/h}$$

does not meet the demand any more, and traffic breaks down at this location. This means, there are now three regions with different flow characteristics:

- Region 1, free traffic upstream of the congestion: Here, the situation is as in Subproblem 1.
- Region 2, congested traffic at and upstream of the bottleneck.
- Region 3, free traffic downstream of the bottleneck.

From the propagation and information velocities of perturbations in free and congested traffic flow, and from the fact that the flow but not the speed derives from a conserved quantity, we can deduce following general rules:

Free traffic flow is controlled by the flow at the upstream boundary, congested traffic flow and the traffic flow downstream of “activated” bottlenecks is controlled by the bottleneck capacity.

For the congested region 2 upstream of the accident (both lanes are available), this means

$$Q_2 = \frac{C_{\text{bottl}}}{2} = 1,008 \text{ vehicles/h}.$$

To determine the traffic density, we invert the flow-density relation of the congested branch of the fundamental diagram,⁴

$$\rho_2 = \rho_{\text{cong}}(Q_2) = \frac{1 - Q_2 T}{l_{\text{eff}}} = 72.5 \text{ vehicles/km}.$$

⁴ *Beware:* The fundamental diagram and derived quantities (as $\rho_{\text{cong}}(Q)$) are always defined for the lane-averaged effective density and flow.

Subproblem 3: To calculate the propagation velocity of the shock (discontinuous transition free \rightarrow congested traffic), we apply the shock-wave formula:

$$c^{\text{up}} = c_{12} = \frac{Q_2 - Q_1}{\rho_2 - \rho_1} = -8.77 \text{ km/h.}$$

Subproblem 4: After lifting the lane closure, the capacity is, again, given by $C = 2Q_{\text{max}} = 4,032$ vehicles/h, everywhere. In the LWR models, the outflow from congestions is equal to the local capacity, so the outflow region 3 is characterized by $Q_3 = C/2 = Q_{\text{max}}$, $V_3 = V_0$, and $\rho_3 = Q_3/V_0 = 20$ vehicles/h. Furthermore, the transition from regions 2 to 3 (downstream jam front) starts to move upstream at a propagation velocity again calculated by the shock-wave formula:

$$c^{\text{down}} = c = c_{23} = \frac{Q_3 - Q_2}{\rho_3 - \rho_2} = -19.2 \text{ km/h.}$$

The jam dissolves if the upstream and downstream jam fronts meet. Defining t as the time past 15:00h, x as in the figure of the problem statement, and denoting the duration of the bottleneck by $\tau_{\text{bottl}} = 30$ min, we obtain following equations of motion for the fronts,

$$\begin{aligned} x_{\text{up}}(t) &= L + c^{\text{up}} t, \\ x_{\text{down}}(t) &= L + c(t - \tau_{\text{bottl}}). \end{aligned}$$

Setting these positions equal results in the time for complete jam dissolution:

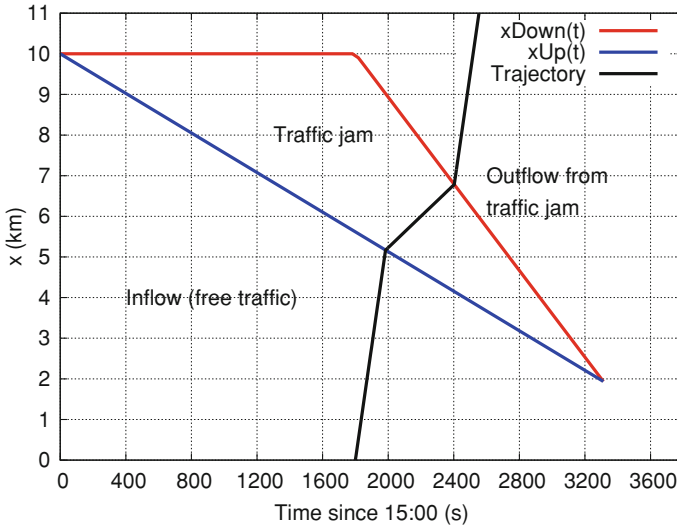
$$t_{\text{dissolve}} = \tau_{\text{bottl}} \frac{c}{c - c^{\text{up}}} = 3,312 \text{ s.}$$

The position of the last vehicle to be obstructed at obstruction time is equal to the location of the two jam fronts when they dissolve:

$$t_{\text{dissolve}} = L + c^{\text{up}} t_{\text{dissolve}} = 1,936 \text{ m.}$$

Subproblem 5: In the spatiotemporal diagram, the congestion is restricted by three boundaries:

- Stationary downstream front at the bottleneck position $L = 10$ km for the times $t \in [0, \tau_{\text{bottl}}]$,
- Moving downstream front for $t \in [\tau_{\text{bottl}}, t_{\text{dissolve}}]$ whose position moves according to $x_{\text{down}}(t) = L + c(t - \tau_{\text{bottl}})$,
- Moving upstream front for $t \in [0, t_{\text{dissolve}}]$ whose position moves according to $x_{\text{up}}(t) = L + c^{\text{up}} t$



Subproblem 6: We follow the vehicle trajectory starting at time $t = t_0 = 1,800$ s at the upstream boundary $x = 0$ by piecewise integrating it through the three regions (cf. the diagram):

1. *Traversing the inflow region:* The vehicle moves at constant speed V_0 resulting in the trajectory $x(t) = V_0(t - t_0)$.
2. *Traversing the jam:* To calculate the time t_{up} of entering the jam, we intersect the free-flow trajectory with the equations of motion $x_{up}(t) = L + c^{up}t$ for the upstream front:

$$t_{up} = \frac{L + V_0 t_0}{V_0 - c^{up}} = 1,984 \text{ s.}$$

The corresponding location $x_{up} = V_0(t_{up} - t_0) = 5,168$ m. Hence, the trajectory reads

$$x(t) = x_{up} + v_{cong}(t - t_{up}), \quad v_{cong} = \frac{Q_2}{\rho_2} = 3.86 \text{ m/s.}$$

3. *Trajectory after leaving the jam:* Since, at time t_{up} , the bottleneck no longer exists, we calculate the exiting time by intersecting the trajectory calculated above with the equations of motion of the moving downstream front. This results in

$$t_{down} = \frac{L - x_{up} - ct_0 + v_{cong}t_{up}}{v_{cong} - c} = 2,403 \text{ s,}$$

$$x_{down} = x_{up} + c_{cong}(t_{down} - t_{up}) = 6,783 \text{ m.}$$

After leaving the jam, the vehicle moves according to trajectory $x(t) = x_{down} + V_0(t - t_{down})$, so the vehicle crosses the location $x = L = 10$ km at time

$$t_{\text{end}} = t_{\text{down}} + \frac{L - x_{\text{down}}}{V_0} = 2,518 \text{ s.}$$

In summary, we obtain for the total travel time to traverse the $L = 10 \text{ km}$ long section

$$\tau = t_{\text{end}} - t_0 = 718.1 \text{ s.}$$

8.6 Jam Propagation on a Highway II: Uphill Grade and Lane Drop

Subproblem 1: As in the previous problem, we calculate the capacities with the capacity formula of the triangular fundamental diagram:

$$Q_{\text{max}} = \frac{V_0}{V_0 T + l_{\text{eff}}} = 2,000 \text{ vehicles/h,}$$

$$Q_{\text{max}}^{\text{III}} = \frac{V_{03}}{V_{03} T_3 + l_{\text{eff}}} = 1,440 \text{ vehicles/h.}$$

Subproblem 2: For the *total* quantities, lane drops, gradients, and other flow-conserving bottlenecks are irrelevant, and the continuity equation reads

$$\frac{\partial \rho_{\text{tot}}}{\partial t} + \frac{\partial Q_{\text{tot}}}{\partial x} = \frac{\partial Q_{\text{tot}}}{\partial x} = 0.$$

Since the inflow is constant, $Q_{\text{in}} = 2,000 \text{ vehicles/h}$, and less the minimum capacity $C^{\text{III}} = 2Q_{\text{max}}^{\text{III}} = 2,880 \text{ vehicles/h}$, this amounts to stationary free traffic flow in all four regions I–IV with $Q_{\text{tot}} = Q_{\text{in}} = \text{const.}$ From this information, we calculate the effective flow of all regions by dividing by the respective number of lanes, and the density by the free part of the fundamental diagram:

	V (km/h)	Q_{tot} (vehicles/h)	Q (vehicles/h/lane)	ρ_{tot} (vehicles/km)	ρ (vehicles/km/lane)
Region I	120	2,000	667	16.7	5.55
Region II	120	2,000	1,000	16.7	8.33
Region III	60	2,000	1,000	33.3	16.7
Region IV	120	2,000	1,000	16.7	8.33

Subproblem 3: Traffic breaks down if the local traffic flow is greater than the local capacity. Thus, the jam forms at a location and at a time where and when this condition is violated, for the first time. Since the capacities in the four regions are given by 6,000, 4,000, 2,880, and 4,000 vehicles/h, respectively, the interface between regions II and III at $x = 3 \text{ km}$ is the first location where the local capacity can no longer meet the new demand $Q_{\text{in}} = 3,600 \text{ vehicles/h}$. Traffic breaks down if the information of

the increased demand reaches $x = 3$ km. This information propagates through the regions I and II at $c_{\text{free}} = V_0 = 120$ km/h, or at 2 km per minute, so

$$x_{\text{breakd}} = 3 \text{ km}, \quad t_{\text{breakd}} = 16:01:30 \text{ h.}$$

Subproblem 4: To determine density, flow, and speed of congested traffic in the regions I and II, we, again, adhere to the rule that free traffic flow is controlled by the upstream boundary while the total flow of congested regions and of regions downstream of “activated” bottlenecks are equal to the bottleneck capacity at some earlier times determined by the information propagation velocities c_{free} and c_{cong} , respectively. Furthermore, densities inside congestions are calculated with the congested branch of the fundamental diagram while the free branch is used in all other cases. Denoting with regions Ib and IIb the congested sections of regions I and II, respectively, and with regions Ia and IIa the corresponding free-flow sections, this leads to following table for the traffic-flow variables:

	V (km/h)	Q_{tot} (vehicles/h)	Q (vehicles/h/lane)	ρ_{tot} (vehicles/km)	ρ (vehicles/km/lane)
Ia ($I = 3$)	16	3,600	1,200	30	10
Ib ($I = 3$)	120	2,880	960	180	60
IIa ($I = 2$)	36	3,600	1,800	30	15
IIb ($I = 2$)	120	2,880	1,440	80	40
III ($I = 2$)	60	2,880	1,440	48	24
IV ($I = 2$)	120	2,880	1,440	24	12

Notice that the local vehicle speed inside congested two-lane regions is more than *twice* that of three-lane regions.⁵

Subproblem 5: To calculate the propagation velocities of the upstream jam front in the regions I and II, we use, again, the shock-wave formula together with the table of the previous subproblem:

$$\begin{aligned}
 v_g &= \frac{\Delta Q}{\Delta \rho} \\
 &= \begin{cases} -240/(60 - 10) \text{ km/h} = -4.8 \text{ km/h} & \text{Interface Ia-Ib, situation (i),} \\ -360/(40 - 15) \text{ km/h} = -14.4 \text{ km/h} & \text{Interface IIa-IIb, situation (ii).} \end{cases}
 \end{aligned}$$

8.7 Diffusion-Transport Equation

Inserting the initial conditions into (8.57) results in

⁵ When being stuck inside jams without knowing the cause, this allows to draw conclusions about the type of bottleneck, e.g., whether it is a three-to-two, or three-to-one lane drop.

$$\rho(x, t) = \rho_0 \int_0^L dx' \frac{1}{\sqrt{4\pi Dt}} \exp \left[\frac{-(x - x' - \tilde{c}t)^2}{4Dt} \right].$$

Since the integrand is formally identical to the density function $f_N(x')$ of a (μ, σ^2) Gaussian distribution (with space and time dependent expectation $\mu(t) = x - \tilde{c}t$ and variance $\sigma^2(t) = 2Dt$), we can the above integral write as⁶

$$\rho(x, t) = \rho_0 \int_0^L dx' f_N^{(\mu, \sigma^2)}(x').$$

Since the integrand is the density of a Gaussian distribution function, the integral itself can be expressed in terms of the (cumulated) Gaussian or normal distribution

$$F_N(x) = \int_{-\infty}^x f_N(x') dx',$$

resulting in

$$\rho(x, t) = \rho_0 \left[F_N^{(\mu, \sigma^2)}(L) - F_N^{(\mu, \sigma^2)}(0) \right].$$

Since this is no elementary function, we express the result in terms of the tabulated standard normal distribution $\Phi(x) = F_N^{(0,1)}(x)$ by using the relation $F(x) = \Phi((x - \mu)/\sigma)$ taught in statistics courses. With $\mu = x - \tilde{c}t$ and $\sigma^2(t) = 2Dt$, this results in

$$\begin{aligned} \rho(x, t) &= \rho_0 \left[\Phi \left(\frac{L - \mu}{\sigma} \right) - \Phi \left(\frac{-\mu}{\sigma} \right) \right] \\ &= \rho_0 \left[\Phi \left(\frac{L - x + \tilde{c}t}{\sqrt{2Dt}} \right) - \Phi \left(\frac{-x + \tilde{c}t}{\sqrt{2Dt}} \right) \right] \\ &= \rho_0 \left[\Phi \left(\frac{x - \tilde{c}t}{\sqrt{2Dt}} \right) - \Phi \left(\frac{x - \tilde{c}t - L}{\sqrt{2Dt}} \right) \right], \end{aligned}$$

In the last line, we have used the symmetry relation $\Phi(x) = 1 - \Phi(-x)$. In the limiting case of zero diffusion, the two standard normal distribution functions degenerate to jump functions with jumps at the positions $\tilde{c}t$ and $L + \tilde{c}t$. This is consistent with the analytic solution of the section-based model, $\rho(x, t) = \rho_0(x - \tilde{c}t)$ where $\rho_0(x)$ denotes the initial density given in the problem statement. For finite diffusion constants, the initially sharp density profiles smear out over time (cf. Fig. 8.26).

⁶ When doing the integral, watch out that the variable to be integrated is x' rather than x .

Problems of Chapter 9

9.1 Ramp Term of the Acceleration Equation

Macroscopically, the total derivative $\frac{dV}{dt}$ of the local speed denotes the rate of change of the average speed of all $n = \rho \Delta x$ vehicles in a (small) road element of length Δx comoving with the local speed V ,

$$\frac{dV}{dt} = \frac{d\langle v_\alpha \rangle}{dt} = \frac{d}{dt} \left(\frac{1}{n} \sum_{\alpha=1}^n v_\alpha \right). \quad (2.4)$$

Without acceleration of single vehicles $\left(\frac{dv_\alpha}{dt} = 0\right)$, the rate of change is solely caused by vehicles entering or leaving this road element at a speed $V_{\text{rmp}} \neq V$ (cf. Fig. 9.5). Assuming that the position of the merging vehicles is uniformly distributed over the length L_{rmp} of the merging region, the rate of change of the vehicle number is given by

$$\frac{dn}{dt} = q = Q_{\text{rmp}} \frac{\Delta x}{L_{\text{rmp}}} \quad (2.5)$$

whenever the moving road element is parallel to the merging section of an on-ramp. When evaluating the time derivative (2.4), we notice that both the prefactor $\frac{1}{n}$ and the sum itself depend explicitly on time. Specifically,

$$\frac{d}{dt} \left(\frac{1}{n} \right) = -\frac{q}{n^2}, \quad \frac{d}{dt} \left(\sum_{\alpha} v_\alpha \right) = q V_{\text{rmp}}.$$

The second equation follows from the problem statement that all vehicles enter the road at speed V_{rmp} and no vehicles (including the ramp vehicles) accelerate ($v_\alpha = \text{const}$). Using these relations and $\sum_{\alpha} v_\alpha = nV$, we can write the rate of change of the local speed as

$$\begin{aligned} A_{\text{rmp}} &= \frac{d\langle v_\alpha \rangle}{dt} = \frac{d}{dt} \left(\frac{1}{n(t)} \sum_{\alpha=1}^{n(t)} v_\alpha \right) \\ &= -\frac{qnV}{n^2} + \frac{qV_{\text{rmp}}}{n} \\ &= \frac{q(V_{\text{rmp}} - V)}{n} \\ &= \frac{Q_{\text{rmp}} \Delta x (V_{\text{rmp}} - V)}{n L_{\text{rmp}}} \\ &= \frac{Q_{\text{rmp}} (V_{\text{rmp}} - V)}{I \rho L_{\text{rmp}}}. \end{aligned}$$

In the last step, we have used $n = I\rho \Delta x$.

9.2 Kinematic Dispersion

Subproblem 1: The lane-averaged local speed is given by

$$V = \frac{1}{\rho_1 + \rho_2} (\rho_1 V_1 + \rho_2 V_2).$$

First, we calculate the initial speed variance across the lanes ($k = 1$ and 2 for the left and right lanes, respectively):

$$\begin{aligned} \sigma_V^2(x, 0) &= \left\langle (V_k(x, 0) - V)^2 \right\rangle \\ &= \frac{\rho_1(V_1 - V)^2 + \rho_2(V_2 - V)^2}{\rho_1 + \rho_2}, \end{aligned}$$

or, for the special case $\rho_1 = \rho_2$,

$$\sigma_V^2(x, 0) = \frac{(V_1 - V_2)^2}{4} = 100 \text{ (m/s)}^2 = \text{const.}$$

Notice that these expressions give the true spatial (instantaneous) variance. In contrast, when determining the time mean variance at a given location from data of a stationary detector station, we would obtain for lane 1 the weighting factor $Q_1/(Q_1 + Q_2) = 1/3$ instead of the correct value $\rho_1/(\rho_1 + \rho_2) = 1/2$ resulting in a biased estimate for the true variance (cf. Chap. 4).

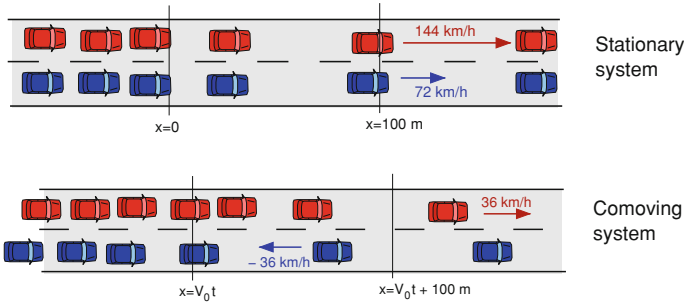
Subproblem 2: The kinematic part $P_{\text{kin}} = \rho \sigma_V^2$ of the pressure term leads to a following contribution of the local macroscopic acceleration,

$$A_{\text{kin}} = -\frac{1}{\rho} \frac{\partial P}{\partial x} = -\frac{1}{\rho} \frac{d}{dx} \left(\rho(x, t) \sigma_V^2 \right) = \begin{cases} \frac{0.01 \text{ s}^{-2}}{\rho} & 0 \leq x \leq 100 \text{ m}, \\ 0 & \text{otherwise.} \end{cases}$$

(The factor 0.01 s^{-2} result from the gradient $\frac{\partial \rho}{\partial x} = 10^{-4} \text{ m}^{-2}$ multiplied by the variance 100 (m/s)^2 .) Consequently, a finite speed variance implies that a negative density gradient leads to a positive contribution of the macroscopic acceleration. This will be discussed at an intuitive level in the next subproblem.

Subproblem 3: If there is a finite variance σ_V^2 and a negative density gradient (a transition from dense to less dense traffic), then the vehicles driving faster than the local speed V go from the region of denser traffic to the less dense region while the slower vehicles are transported backwards (in the comoving system!) to the denser region. Due to the density gradient, the net inflow of faster vehicles is positive and

that of slower vehicles negative. This is illustrated in the following figure, the upper graphics of which depicting the situation in the stationary system, and the lower one in a system comoving with V . As a result, the averaged speed V is increasing although *not a single vehicle* accelerates while the total number of vehicles in the element, i.e., the density, is essentially constant.



Subproblem 4: Assuming that higher actual speeds are positively correlated with higher desired speeds, the mechanism described in Subproblem 3 leads to a *segregation* of the desired speeds such that the fast tail of the desired speed distribution tends to be found further downstream than the slow tail. This is most conspicuous in multi-lane queues of city traffic waiting behind a red traffic light when the light turns green: If there is one lane with speeding drivers, these drivers will reach first a given position downstream of the stopping line of the traffic light. At this moment, the traffic composition at this point consists exclusively of speeding drivers. Macroscopically, this can only be modeled by multi-class macroscopic models where the desired speed $V_0(x, t)$ becomes another dynamical field with its own dynamical equation. Because of their complexity, such *Paveri-Fontana models* are rarely used.

9.3 Modeling Anticipation by Traffic Pressure

Subproblem 1: Since, by definition, the traffic density is equal to the number of vehicles per distance, one vehicle distance, i.e., the distance headway d , can be expressed by the density:

$$d = \frac{1}{\rho((x + x_a)/2, t)} \approx \frac{1}{\rho(x, t)}.$$

The first expression to the right of the equal sign is accurate to second order in $x_a - x = d$. The second expression $1/\rho(x, t)$ is accurate to first order which is sufficient in the following.

Subproblem 2: We expand the nonlocal part $V_e(\rho(x_a, t)) = V_e(\rho(x + d, t))$ of the adaptation term to first order around x :

$$\begin{aligned}
 V_e(\rho(x+d, t)) &= V_e(\rho(x, t)) + \frac{dV_e(\rho(x, t))}{dx} d + \mathcal{O}(d^2) \\
 &= V_e(\rho(x, t)) + \frac{1}{\rho} \frac{dV_e(\rho(x, t))}{dx} + \mathcal{O}(d^2).
 \end{aligned}$$

Inserting this into the speed adaptation term results in

$$\begin{aligned}
 \left(\frac{dV}{dt} \right)_{\text{relax+antic}} &\approx \frac{V_e(\rho(x, t)) - V(x, t)}{\tau} + \frac{1}{\rho \tau} \frac{dV_e(\rho(x, t))}{dx} \\
 &\stackrel{!}{=} \frac{V_e(\rho(x, t)) - V(x, t)}{\tau} - \frac{1}{\rho} \frac{dP(x, t)}{dx},
 \end{aligned}$$

where, in the last step, we set the result equal to the general expression for the acceleration caused by P . The comparison yields

$$P(x, t) = -\frac{V_e(\rho(x, t))}{\tau}.$$

Subproblem 3: According to the problem statement, the density profile obeys (with $\rho_0 = 20$ vehicles/km $= 0.02$ vehicle/m, $c = 100$ vehicles/km² $= 10^{-4}$ vehicle/m²)

$$\rho(x, t) = \begin{cases} \rho_0 & x < 0, \\ \rho_0 + cx & 0 < x \leq 200 \text{ m}, \\ 2\rho_0 & x > 200 \text{ m}. \end{cases} \quad (2.6)$$

(i) Acceleration by anticipation when using the original relaxation term:

$$\left(\frac{dV}{dt} \right)_{\text{relax}} = \frac{V_e(\rho(x + 1/\rho(x, t), t)) - V_e(\rho(x, t))}{\tau},$$

where $V_e(\rho) = V_0(1 - \rho/\rho_{\max})$ is given in the problem statement (such a relation is rather unrealistic; it serves to show the principle in the easiest possible way). Inserting Eq. (2.6), we obtain

$$\left(\frac{dV}{dt} \right)_{\text{relax}} = \begin{cases} 0 & x \leq -1/\rho_0 \text{ or } x > 200 \text{ m}, \\ \frac{-V_0 c}{\tau \rho_{\max}} \left(\frac{1}{\rho_0} + x \right) & -\frac{1}{\rho_0} < x \leq 0, \\ \frac{-V_0 c}{\tau \rho_{\max} \rho} & 0 < x \leq 200 \text{ m} - \frac{1}{2\rho_0}, \\ \frac{-V_0}{\tau \rho_{\max}} (2\rho_0 - \rho) & 200 \text{ m} - \frac{1}{2\rho_0} < x \leq 200 \text{ m}, \end{cases}$$

where the criterion separating the last two cases is only approximatively valid.

(ii) Expressing the acceleration contribution by the pressure term, we obtain

$$\left(\frac{dV}{dt}\right)_{\text{pressure}} = \begin{cases} 0 & x \leq 0 \text{ or } x > 200 \text{ m}, \\ \frac{-V_0 c}{\tau \rho_{\max} \rho} & 0 < x \leq 200 \text{ m} - \frac{1}{2\rho_0}. \end{cases}$$

Except for the transition regions at the beginning and end of the density gradient, this agrees with the acceleration derived from the original relaxation term. However, in contrast to the pressure term, the nonlocal anticipation term provides “true” anticipation everywhere, including the region $-1/\rho_0 \leq x < 0$ where the local approximation by the pressure term does not “see” anything. In summary, the non-local route to modeling anticipation is more robust.

9.4 Steady-State Speed of the GKT Model

In the steady state on homogeneous roads, all spatial and temporal derivatives vanish, so the GKT acceleration equation (9.24) reduces to $V = V_e^*$. Furthermore, the homogeneity associated with the steady state implies $V_a = V$ and $\rho_a = \rho$, and the Boltzmann factor is given by $B(0) = 1$. Using these conditions and the definition (9.27) for V_e^* , we can write the condition $V = V_e^*$ as

$$\frac{V}{V_0} = 1 - \frac{\alpha(\rho)}{\alpha(\rho_{\max})} \left(\frac{\rho_a V T}{1 - \rho_a / \rho_{\max}} \right)^2.$$

This is a quadratic equation in V . Its positive root reads

$$V = V_e(\rho) = \frac{\tilde{V}^2}{2V_0} \left(-1 + \sqrt{1 + \frac{4V_0^2}{\tilde{V}^2}} \right)$$

with the abbreviation

$$\tilde{V} = \sqrt{\frac{\alpha(\rho_{\max})}{\alpha(\rho)} \frac{(1 - \rho/\rho_{\max})}{\rho T}}.$$

For densities near the maximum density we have $\tilde{V} \ll V_0$ and $\alpha(\rho) \approx \alpha(\rho_{\max})$. With the micro-macro relation $s = 1/\rho - 1/\rho_{\max}$, we can write the steady-state speed in this limit as

$$V_e(\rho) \approx \tilde{V} \approx \frac{(1 - \rho/\rho_{\max})}{\rho T} = \frac{s}{T}.$$

Notice that this implies that T has the meaning of a (bumper-to-bumper) time gap in heavily congested traffic.

9.5 Flow-Conserving form of Second-Order Macroscopic Models

We start by setting $V = Q/\rho$ in the continuity equation:

$$\frac{\partial \rho}{\partial t} + \frac{\partial Q}{\partial x} = -\frac{Q}{I} \frac{dI}{dx} + v_{\text{rmp}}.$$

Multiplying the acceleration equation (9.11) by ρ and inserting $V = Q/\rho$ gives the intermediate result

$$\rho \frac{\partial V}{\partial t} + Q \frac{\partial V}{\partial x} = \frac{\rho V_e^* - Q}{\tau} - \frac{\partial P}{\partial x} + \frac{\partial}{\partial x} \left(\eta \frac{\partial(Q/\rho)}{\partial x} \right) + \rho A_{\text{rmp}}.$$

Now we substitute the time derivative of the local speed by a time derivative of the flow. The left-hand side of the last equation then reads

$$\begin{aligned} \rho \frac{\partial V}{\partial t} + Q \frac{\partial V}{\partial x} &= \frac{\partial Q}{\partial t} - V \frac{\partial \rho}{\partial t} + Q \frac{\partial V}{\partial x} \\ &= \frac{\partial Q}{\partial t} + V \frac{\partial Q}{\partial x} + V \frac{Q}{I} \frac{dI}{dx} - V v_{\text{rmp}} + Q \frac{\partial V}{\partial x} \\ &= \frac{\partial Q}{\partial t} + \frac{\partial(QV)}{\partial x} + V \frac{Q}{I} \frac{dI}{dx} - V v_{\text{rmp}}. \end{aligned}$$

Substituting again $V = Q/\rho$ and grouping the spatial derivatives together, we obtain

$$\frac{\partial Q}{\partial t} + \frac{\partial}{\partial x} \left[\frac{Q^2}{\rho} + P - \eta \frac{\partial}{\partial x} \left(\frac{Q}{\rho} \right) \right] = \frac{\rho V_e^* - Q}{\tau} + \frac{Q^2}{\rho I} \frac{dI}{dx} - \frac{Q v_{\text{rmp}}}{\rho} + \rho A_{\text{rmp}}.$$

9.6 Numerics of the GKT Model

Neglecting the pressure term (its maximum relative influence is of the order of $\sqrt{\alpha} = 10\%$), the first CFL condition (9.39) for the convective numerical instability reads

$$\Delta t < \frac{\Delta x}{V_0} = 1.5 \text{ s}. \quad (2.7)$$

Since the GKT model does not contain diffusion terms, the second CFL condition is not relevant. However, the relaxation instability must be tested: The characteristic equation $\det(\underline{L} - \lambda \underline{I}) = 0$ for the eigenvalues of the matrix \underline{L} of the linear equation (9.36) reads

$$-\lambda(L_{22} - \lambda) = -\lambda \left[\frac{1}{\tau} \left(-1 + \rho \frac{\partial \tilde{V}_e(\rho, Q)}{\partial Q} \right) - \lambda \right] = 0$$

resulting in the eigenvalues

$$\lambda_1 = 0, \quad \lambda_2 = -\frac{1}{\tau} \left(1 - \rho \frac{\partial \tilde{V}_e(\rho, Q)}{\partial Q} \right),$$

where

$$\tilde{V}_e(\rho, Q) = V_e^*(\rho, Q, \rho, Q) = V_0 \left[1 - \frac{\alpha(\rho)}{\alpha_{\max}} \left(\frac{Q_e T}{1 - \rho/\rho_{\max}} \right)^2 \right].$$

With this result, the condition $\Delta t < |\lambda_2^{-1}|$ to avoid relaxation instability becomes

$$\Delta t < \frac{\tau}{1 + \frac{2\alpha(\rho)V_0\rho Q_e}{\alpha_{\max}} \left(\frac{T}{1 - \rho/\rho_{\max}} \right)^2},$$

i.e., Eq. (9.44) of the main text. In the limit of high densities $\rho \approx \rho_{\max}$ we make use of the approximate relation (cf. Problem 9.4)

$$V_e(\rho) \approx \frac{1}{T} \left(\frac{1}{\rho} - \frac{1}{\rho_{\max}} \right)$$

to arrive at

$$\Delta t \left(1 + 2 \frac{V_0}{V_e} \right) < \tau$$

which is Eq. (9.45) of the main text. Inserting $\rho_{\max, \text{sim}} = 0.1 \text{ m}^{-1}$ from the problem statement and $V_e(\rho_{\max, \text{sim}}) = 4.14 \text{ m/s}$ (watch out for the units! If in doubt, always use the SI units m, kg, and s), we finally obtain

$$\Delta t < \frac{1}{|\lambda_2|} = 1.32 \text{ s}. \quad (2.8)$$

The definitive limitation of the time step is given by the more restrictive one of the conditions (2.7) and (2.8), so $\Delta t < 1.32 \text{ s}$.

The expression (9.48) for the numerical diffusion of both equations at $V = 20 \text{ m/s}$ and $\Delta t = 1 \text{ s}$ (i.e., the conditions for linear numerical stability are satisfied) evaluates to

$$D_{\text{num}} = V \frac{\Delta x}{2} \left(1 - V \frac{\Delta t}{\Delta x} \right) = 300 \text{ m/s}^2.$$

This is only about 1/30 of the (real) diffusion introduced to the Kerner-Konhäuser model by the term proportional to D_v (assuming standard parameterization).

Problems of Chapter 10

10.1 Dynamics of a Single Vehicle Approaching a Red Traffic Light

Subproblem 1 (parameters). The free acceleration is the same as that of the OVM. Hence, v_0 is the desired speed and τ the adaptation time. If the model decelerates, it does so with the deceleration b . Since, at this deceleration, the kinematic braking distance to a complete stop is given by $\Delta x_{\text{brake}} = v^2/(2b)$, the vehicle stops at a distance s_0 to the (stopping line of) the red traffic light. This explains the meaning of the last parameter. Notice that, in this model, vehicles would follow any leading vehicle driving at a constant speed $v_l < v_0$ at the same gap s_0 , i.e., the model does not include a safe gap. Nor does it contain a reaction time. The model is accident-free with respect to stationary obstacles, but not when slower vehicles are involved.

Subproblem 2 (acceleration). Here, the first condition of the model applies, so we have to solve the ordinary differential equation (ODE) for the speed

$$\frac{dv}{dt} = \frac{v_0 - v}{\tau} \quad \text{with } v(0) = 0.$$

The exponential ansatz $e^{\lambda t}$ for the homogeneous part $\frac{dv}{dt} = -v/\tau$ gives the solvability condition $\lambda = 1/\tau$. Furthermore, the general solution for the full inhomogeneous ODE reads

$$v(t) = Ae^{-t/\tau} + B.$$

The asymptotic $v(\infty) = B = v_0$ yields the inhomogeneous part B . Determining the integration constant A by the initial condition $v(0) = A + B = A + v_0 = 0$ gives $A = -v_0$, so the speed profile reads

$$v(t) = v_0 \left(1 - e^{-t/\tau}\right).$$

Once $v(t)$ is known, we determine the trajectory $x(t)$ by integrating over time. With $x(0) = 0$, we obtain

$$\begin{aligned} x(t) &= \int_0^t v(t') dt' = v_0 \int_0^t \left(1 - e^{-t'/\tau}\right) dt' \\ &= v_0 \left[t' + \tau e^{-t'/\tau} \right]_{t'=0}^{t'=t} = v_0 t + v_0 \tau \left(e^{-t/\tau} - 1 \right). \end{aligned}$$

By identifying parts of this expression with $v(t)$, this simplifies to

$$x(t) = v_0 t - v(t)\tau.$$

Finally, to obtain the acceleration profile, we either differentiate $v(t)$, or insert $v(t)$ into the right-hand side of the ODE. In either case, the result is

$$\dot{v} = \frac{v_0 - v}{\tau} = \frac{v_0}{\tau} e^{-t/\tau}.$$

Subproblem 3 (braking phase). The red traffic light represents a standing virtual vehicle of zero length at the stopping line, so $\Delta v = v$. This phase starts at a distance

$$s_c = s_0 + \frac{v^2}{2b} = 50.2 \text{ m}$$

to the stopping line, and the vehicle stops at a distance s_0 to this line.

Subproblem 4 (trajectory). For the accelerating phase, the trajectory has already been calculated. The deceleration phase begins at the location

$$x_c = L - s_c = L - s_0 - \frac{v^2}{2b} \approx 450 \text{ m}.$$

To approximatively determine the time t_c at which the deceleration phase begins, we set $v(t_c) = v_0$ to obtain

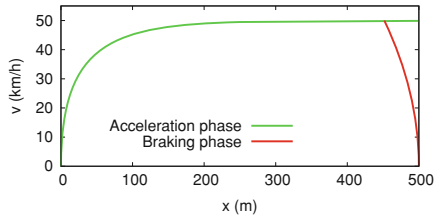
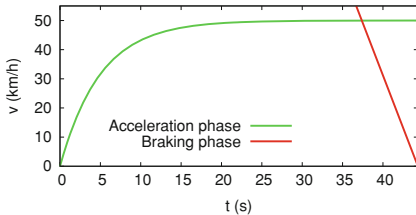
$$x_c(t_c) = v_0 t_c - v(t_c)\tau \approx v_0(t_c - \tau) \Rightarrow t_c = \frac{x_c}{v_0} + \tau = 32.4 \text{ s} + 5.0 \text{ s} = 37.4 \text{ s}.$$

With the braking time v_0/b , this also gives the stopping time

$$t_{\text{stop}} = t_c + \frac{v_0}{b} = 44.3 \text{ s}.$$

In summary, the speed profile $v(t)$ can be expressed by (cf. the graphics below)

$$v(t) = \begin{cases} v_0 (1 - e^{-t/\tau}) & 0 \leq t < t_c, \\ v_0 - b(t - t_c) & t_c \leq t \leq t_{\text{stop}}, \\ 0 & \text{otherwise.} \end{cases}$$



10.2 OVM Acceleration on an Empty Road

(i) The maximum acceleration $a_{\max} = v_0/\tau$ is reached right at the beginning, $t = 0$. (ii) Prescribing $a_{\max} = 2 \text{ m/s}^2$ and a desired speed $v_0 = 120 \text{ km/h}$ determines the speed relaxation time by

$$\tau = \frac{v_0}{a_{\max}} = 16.7 \text{ s}.$$

(iii) We require that, at a time t_{100} to be determined, the speed should reach the value $v_{100} = 100 \text{ km/h}$:

$$v(t_{100}) = v_{100} = v_0 \left(1 - e^{-\frac{t_{100}}{\tau}}\right).$$

Solving this condition for t_{100} gives

$$\frac{v_{100}}{v_0} = 1 - e^{-\frac{t_{100}}{\tau}} \Rightarrow t_{100} = -\tau \ln \left(1 - \frac{100}{120}\right) \approx 29.9 \text{ s}.$$

10.3 Optimal Velocity Model on a Ring Road

The problem describes a situation with evenly spaced identical vehicles on a ring road which, initially, are at rest. This means, traffic flow is not stationary (since the initial gaps are greater than the minimum gap) but homogeneous: Since the road is homogeneous, and the vehicle fleet consists of identical vehicles, the homogeneity imposed by the initial conditions is not destroyed over time. For microscopic models, homogeneity implies that the dynamics depend neither on x nor on the vehicle index α . So, dropping α , the OVM reads

$$\frac{dv}{dt} = \frac{v_{\text{opt}}(s(0)) - v}{\tau}.$$

The solution to this ODE is analogously to Problem 10.2, only v_0 is replaced by the steady-state speed $v_e = v_{\text{opt}}(s(0))$.

10.4 Full Velocity Difference Model

General plausibility arguments require the steady-state speed $v_{\text{opt}}(s)$ to approach the desired speed v_0 when the gap s tends to infinity. However, for an arbitrarily large distance to the red traffic light modeled by a standing virtual vehicle ($\Delta v = v$), the FVDM vehicle accelerates according to

$$\dot{v} = \frac{v_0 - v}{\tau} - \lambda v = \frac{v_0}{\tau} - \left(\frac{1}{\tau} + \lambda\right) v.$$

From this it follows that the acceleration \dot{v} becomes zero for a terminal speed

$$v^* = \frac{v_0}{1 + \lambda \tau}.$$

This is the maximum speed an initially standing Full Velocity Difference Model (FVDM) vehicle can reach in this situation. It is significantly lower than v_0 . For the parameter values of the problem statement, $v^* = 13.5$ km/h which agrees with Fig. 10.6.

10.5 A Simple Model for Emergency Braking Maneuvers

Subproblem 1 (identifying the parameters). T_r denotes the reaction time, and b_{\max} is the maximum deceleration in emergency cases.

Subproblem 2 (braking and stopping distance). Assuming a fixed reaction timer T_r and a constant deceleration b_{\max} in the braking phase, elementary kinematic relations yield following expressions for the braking and stopping distances $s_B(v)$ and $s_{\text{stop}}(v) = vT_r + s_B(v)$, respectively:

$$s_B(v) = \frac{v^2}{2b_{\max}}, \quad s_{\text{stop}}(v) = vT_r + s_B(v)$$

with the numerical values

$$\begin{aligned} v = 50 \text{ km/h} : \quad s_B(v) &= 12.1 \text{ m}, \quad s_{\text{stop}}(v) = 25.9 \text{ m}, \\ v = 70 \text{ km/h} : \quad s_B(v) &= 23.6 \text{ m}, \quad s_{\text{stop}}(v) = 43.1 \text{ m}. \end{aligned}$$

Subproblem 3 (emergency braking). At first, we determine the initial distance such that a driver driving at $v_1 = 50$ km/h just manages to stop before hitting the child:

$$s(0) = s_{\text{stop}}(v_1) = 25.95 \text{ m}.$$

Now we consider a speed $v_2 = 70$ km/h but the same initial distance $s(0) = 25.95$ m as calculated above. At the end of the reaction time, the child is just

$$s(T_r) = s(0) - v_2 T_r = 6.50 \text{ m}$$

away from the front bumper. Now, the driver would need the additional braking distance $s_B(v_2) = 23.6$ m for a complete stop. However, only 6.50 m are available resulting in a difference $\Delta s = 17.13$ m. With this information, the speed at collision can be calculated by solving $\Delta s = (\Delta s)_B(v) = v^2/(2b_{\max})$ for v , i.e.,

$$v_{\text{coll}} = \sqrt{2b_{\text{max}}\Delta s} = 16.56 \text{ m/s} = 59.6 \text{ km/h.}$$

Remark This problem stems from a multiple-choice question of the theoretical exam for a German driver's licence. The official answer is 60 km/h.

Problems of Chapter 11

11.1 Conditions for the Microscopic Fundamental Diagram

The plausibility condition (11.5) is valid for any speed v_l of the leading vehicle. This also includes standing vehicles where Eq. (11.5) becomes $a_{\text{mic}}(s, 0, 0) = 0$ for $s \leq s_0$. This corresponds to the steady-state condition $v_e(s) = 0$ for $s \leq s_0$.

Conditions (11.1) and (11.2) are valid for any speed v_l of the leader as well, including the steady-state situation $v_l = v$ or $\Delta v = 0$. For the alternative acceleration function $\tilde{a}(s, v, \Delta v)$, this means

$$\frac{\partial \tilde{a}(s, v, 0)}{\partial s} \geq 0, \quad \frac{\partial \tilde{a}(s, v, 0)}{\partial v} < 0.$$

Along the one-dimensional manifold of steady-state solutions $\{v_e(s)\}$ for $s \in [0, \infty[$, we have $\tilde{a}(s, v_e(s), 0) = 0$, so the differential change $d\tilde{a}$ along the equilibrium curve $v_e(s)$ must vanish as well:

$$d\tilde{a} = \frac{\partial \tilde{a}(s, v_e(s), 0)}{\partial s} ds + \frac{\partial \tilde{a}(s, v_e(s), 0)}{\partial v} v'_e(s) ds = 0,$$

hence

$$v'_e(s) = \frac{-\partial \tilde{a}(s, v, 0)/\partial s}{\partial \tilde{a}(s, v, 0)/\partial v} \geq 0.$$

If the leading vehicle is outside the interaction range, we have $v'_e(s) = 0$ [second condition of Eq. (11.2)]. Finally, the condition $\lim_{s \rightarrow \infty} v_e(s) = v_0$ follows directly from the second part of condition (11.1).

11.2 Rules of Thumb for the Safe Gap and Braking Distance

Subproblem 1. One mile corresponds to 1.609 km. However, the US rule does not give explicit values for a vehicle length. Here, we assume 15 ft = 4.572 m. In any case, the gap s increases linearly with the speed v , so the time gap $T = s/v$ is independent

of speed. Implementing this rule, we obtain

$$T = \frac{s}{v} = \frac{15\text{ft}}{10\text{mph}} = \frac{4.572\text{ m}}{16.09\text{ km/h}} = \frac{4.572\text{ m}}{4.469\text{ m/s}} = 1.0\text{ s}.$$

Notice that, in the final result, we rounded off generously. After all, this is a rule of thumb and more significant digits would feign a non-existent precision.⁷ Notice that this rule is consistent with typically observed gaps (cf. Fig. 4.8).

Subproblem 2. Here, the speedometer reading is in units of km/h, and the space gap is in units of meters. Again, the quotient, i.e., the time gap T is constant and given by (watch out for the units)

$$T = \frac{s}{v} = \frac{\frac{1}{2}\text{m}\left(\frac{v}{\text{km/h}}\right)}{v} = \frac{\frac{1}{2}\text{m}}{\text{km/h}} = \frac{0.5\text{ h}}{1,000} = \frac{1,800\text{ s}}{1,000} = 1.8\text{ s}.$$

Subproblem 3. The kinematic *braking distance* is $s(v) = v^2/(2b)$, so the cited rule of thumb implies that the braking deceleration does not depend on speed. By solving the kinematic braking distance for b and inserting the rule, we obtain (again, watch out for the units)

$$b = \frac{v^2}{2s} = \frac{v^2}{0.02\text{ m}} \left(\frac{\text{km}}{\text{h}}\right)^2 = \frac{50}{3.6^2} \text{ m/s}^2 = 3.86 \text{ m/s}^2.$$

For reference, comfortable decelerations are below 2 m/s^2 while emergency braking decelerations on dry roads with good grip conditions can be up to 10 m/s^2 , about 6 m/s^2 for wet conditions, and less than 2 m/s^2 for icy conditions. This means, the above rule could lead to accidents for icy conditions but is okay, otherwise.

11.3 Reaction to Vehicles Merging into the Lane

Reaction for the IDM. For $v = v_0/2$, the IDM steady-state space gap reads

$$s_e(v) = \frac{s_0 + vT}{\sqrt{1 - \left(\frac{v}{v_0}\right)^\delta}} = \frac{s_0 + \frac{v_0 T}{2}}{\sqrt{1 - \left(\frac{1}{2}\right)^\delta}}.$$

The prevailing contribution comes from the prescribed time headway (for $s_0 = 2 \text{ m}$ and $\delta = 4$, the other contributions only make up about 10 %). This problem assumes that the merging vehicle reduces the gap to the considered follower to half the steady-

⁷ There is also a more conservative variant of this rule where one should leave one car length every five mph corresponding to the “two-second rule” $T = 2.0 \text{ s}$.

state gap, $s = s_e/2 = v_0 T/4$, while the speed difference remain zero. The new IDM acceleration of the follower (with $a = 1 \text{ m/s}^2$ and $\delta = 4$) is therefore

$$\begin{aligned} \dot{v}_{\text{IDM}} &= a \left[1 - \left(\frac{v}{v_0} \right)^\delta - \left(\frac{s_0 + vT}{s} \right)^2 \right] \\ &\stackrel{(v=v_0/2, s=s_e/2)}{=} a \left[1 - \left(\frac{1}{2} \right)^\delta - \left(\frac{s_0 + v_0 T/2}{s_e/2} \right)^2 \right] \\ &\stackrel{s_e(v)=s_e(v_0/2)}{=} -3a \left[1 - \left(\frac{1}{2} \right)^\delta \right] = -\frac{45}{16} \text{ m/s}^2 = -2.81 \text{ m/s}^2. \end{aligned}$$

Reaction for the simplified Gipps' model. For this model, the steady-state gap in the car-following regime reads $s_e(v) = v \Delta t$. Again, at the time of merging, the merging vehicle has the same speed $v_0/2$ as the follower, and the gap is half the steady-state gap, $s = (v \Delta t)/2 = v_0 \Delta t/4$. The new speed of the follower is restricted by the safe speed v_{safe} :

$$v(t + \Delta t) = v_{\text{safe}} = -b \Delta t + \sqrt{b^2 (\Delta t)^2 + \left(\frac{v_0}{2} \right)^2 + \frac{b v_0 \Delta t}{2}} = 19.07 \text{ m/s}.$$

This results in an effective acceleration

$$\left(\frac{dv}{dt} \right)_{\text{Gipps}} = \frac{v(t + \Delta t) - v(t)}{\Delta t} \approx -0.93 \text{ m/s}^2.$$

We conclude that the Gipps' model describes a more relaxed driver reaction compared to the IDM. Notice that both the IDM and Gipps' model would generate significantly higher decelerations for the case of slower leading vehicles (dangerous situation).

11.4 The IDM Braking Strategy

A braking strategy is self-regulating if, during the braking process, the *kinematically necessary deceleration* $b_{\text{kin}} = v^2/(2s)$ approaches the comfortable deceleration b . In order to show this, we calculate the rate of change of the kinematic deceleration (applying the quotient and chain rules of differentiation when necessary) and set $\dot{s} = -v$ and $\dot{v} = -b_{\text{kin}}^2/b = -v^4/(4bs^2)$, afterwards. This eventually gives Eq. (11.19) of the main text:

$$\begin{aligned} \frac{db_{\text{kin}}}{dt} &= \frac{d}{dt} \left(\frac{v^2}{2s} \right) = \frac{4vs\dot{v} - 2v^2\dot{s}}{4s^2} \\ &= \frac{v^3}{2s^2} \left(1 - \frac{v^2}{2sb} \right) = \frac{v}{s} \frac{b_{\text{kin}}}{b} (b - b_{\text{kin}}), \end{aligned}$$

11.5 Analysis of a Microscopic Model

Subproblem 1 (parameters). For interaction-free accelerations, $v_{\text{safe}} > v_0$, so v_{safe} is not relevant. Hence v_0 denotes the desired speed, and a the absolute value of the acceleration and deceleration for the cases $v < v_0$ and $v > v_0$, respectively. The steady-state conditions $s = \text{const.}$ and $v = v_l = v_e = \text{const.}$ give

$$v_e = \min(v_0, v_{\text{safe}}).$$

Without interaction, $v_{\text{safe}} > v_0$, so $v_e = v_0$. With interactions, the safe speed becomes relevant and the above condition yields

$$v_e = v_{\text{safe}} = -aT + \sqrt{a^2T^2 + v_e^2 + 2a(s - s_0)}$$

which can be simplified to

$$s = s_0 + v_e T.$$

Thus, s_0 is the minimum gap for $v = 0$, and T the desired time gap. The model produces a deceleration $-a$ not only if $v > v_0$ (driving too fast in free traffic) but also if $v > v_{\text{safe}}$ (driving too fast in congested situations). Furthermore, the model is symmetrical with respect to accelerations and decelerations. Obviously, it is not accident free.

Subproblem 2 (steady-state speed). We have already derived the steady-state condition

$$v_e(s) = \min\left(v_0, \frac{s - s_0}{T}\right).$$

Macroscopically, this corresponds to the triangular fundamental diagram

$$Q_e(\rho) = \min\left(v_0\rho, \frac{1 - \rho l_{\text{eff}}}{T}\right)$$

where $l_{\text{eff}} = 1/\rho_{\text{max}} = l + s_0$. The capacity per lane is given by $Q_{\text{max}} = (T + l_{\text{eff}}/v_0)^{-1} = 1,800$ vehicles/h at a density $\rho_C = 1/(l_{\text{eff}} + v_0T) = 25/\text{km}$. For further properties of the triangular fundamental diagram, see Sect. 8.5.

Subproblem 3. The acceleration and braking distances to accelerate from 0 to 20 m/s or to brake from 20 m/s to 0, respectively, are the same:

$$s_a = s_b = \frac{v_0^2}{2a} = 200 \text{ m.}$$

At a minimum gap of 3 m and the location $x_{\text{stop}} = 603 \text{ m}$ of the stopping line of the traffic light, the acceleration takes place from $x = 0$ to $x_1 = 200 \text{ m}$, and the deceleration from $x_2 = 400 \text{ m}$ to $x_3 = 600 \text{ m}$. The duration of the acceleration and deceleration phases is $v_0/a = 20 \text{ s}$ while the time to cruise the remaining stretch of 200 m at v_0 amounts to 10 s. This completes the information to mathematically describe the trajectory:

$$x(t) = \begin{cases} \frac{1}{2}at^2 & t \leq t_1 = 20 \text{ s}, \\ x_1 + v_0(t - t_1) & t_1 < t \leq t_2 = 30 \text{ s}, \\ x_2 + v_0(t - t_2) - \frac{1}{2}a(t - t_2)^2 & t_2 < t \leq t_3 = 50 \text{ s}, \end{cases}$$

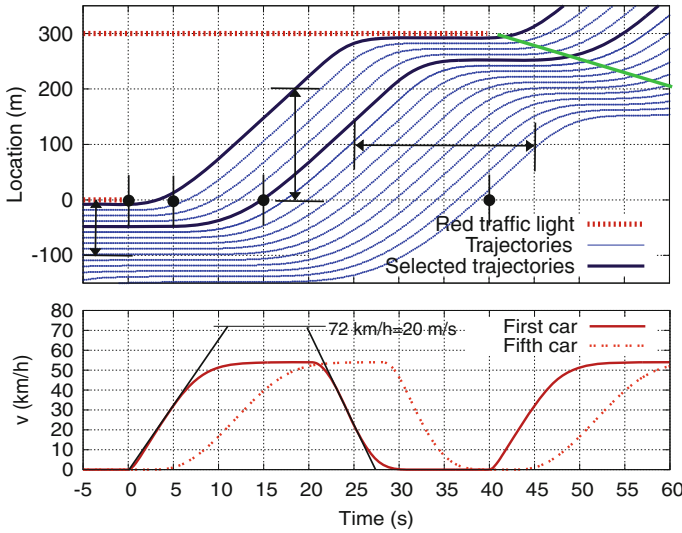
where $t_1 = 20 \text{ s}$, $t_2 = 30 \text{ s}$ and $t_3 = 50 \text{ s}$.

11.6 Heterogeneous Traffic

The simultaneous effects of heterogeneous traffic and several lanes with lane-changing and overtaking possibilities results in a curved free part of the fundamental diagram even for models that would display a triangular fundamental diagram for identical vehicles and drivers (as the Improved Intelligent Driver Model, IIDM). This can be seen as follows: For heterogeneous traffic, each vehicle-driver class has a different fundamental diagram. Particularly, the density ρ_C at capacity is different for each class, so a simple weighted average of the individual fundamental diagrams would result in a curved free part and a rounded peak. However, without lane-changing and overtaking possibilities, all vehicles would queue up behind the vehicles of the slowest class resulting in a straight free part of the fundamental diagram with the gradient representing the lowest free speed.⁸ So, both heterogeneity and overtaking possibilities are necessary to produce a curved free part of the fundamental diagram.

⁸ Even when obstructed, drivers can choose their preferred gap (in contrast to the desired speed), so the congested branch of the fundamental diagram is curved even without overtaking possibilities.

11.7 City Traffic in the Improved IDM



1. For realistic circumstances, the maximum possible flow is given by the *dynamic* capacity, i.e., the outflow from moving downstream congestion fronts. In our case, the “congestion” is formed by the queue of standing vehicles behind a traffic light. Counting the trajectories (horizontal double-arrow in the upper diagram) yields

$$C = Q_{\max} \approx \frac{9 \text{ vehicles}}{20 \text{ s}} = 1,620 \text{ vehicles/h.}$$

2. Counting the trajectories passing $x = 0$ for times less than 5, 15, and 40 s (black bullets in the upper diagram) gives

$$n(5) = 1, \quad n(15) = 5, \quad n(40) = 15,$$

respectively. We determine β by the average time headway after the first vehicles have passed,

$$\beta = \frac{1}{C} = \frac{40 \text{ s} - 15 \text{ s}}{15 - 5} = 2.5 \text{ s/vehicles.}$$

We observe, that β denotes the inverse of the capacity. The obtained value agrees with the result of the first subproblem within the “measuring uncertainty” of one vehicle.⁹ This also gives the *additional time* until the first vehicle passes: $\tau_0 = 15 \text{ s} - 5\beta = 2.5 \text{ s}$. (Notice that this is *not* a reaction time since the IIDM does not have one.)

⁹ One could have calculated β as well using the pairs $\{n(15), n(5)\}$ or $\{n(40), n(5)\}$ with similar results.

3. The propagation velocity of the position of the starting vehicles in the queue is read off from the upper diagram:

$$c_{\text{cong}} = -\frac{100 \text{ m}}{20 \text{ s}} = -5 \text{ m/s} = -18 \text{ km/h.}$$

4. We estimate the desired speed by the maximum speed of the speed profile (lower diagram): $v_0 = 15 \text{ m/s} = 54 \text{ km/h}$. The effective length l_{eff} is equal to the distance between the standing vehicles in the upper diagram: $\rho_{\text{max}} = 1/l_{\text{eff}} = 10 \text{ vehicles/100 m} = 100 \text{ vehicles/km}$, i.e., $l_{\text{eff}} = 10 \text{ m}$. Since the steady state of this model corresponds to a triangular fundamental diagram, the time gap parameter T is determined by the propagation speed and the maximum density: $T = -l_{\text{eff}}/c = 2 \text{ s}$. Finally, the maximum acceleration a and the comfortable deceleration b can be read off the lower diagram by estimating the maximum and minimum gradient of the speed profile:

$$a = \frac{20 \text{ m/s}}{10 \text{ s}} = 2 \text{ m/s}^2, \quad b = \frac{20 \text{ m/s}}{7 \text{ s}} = 2.9 \text{ m/s}^2.$$

Problems of Chapter 12

12.1 Statistical Properties of the Wiener Process

To determine the expectation $\langle w(t)w(t') \rangle$ from the given formal solution $w(t)$ to the stochastic differential equation of the Wiener process, we insert the formal solution into $\langle w(t)w(t') \rangle$ carefully distinguishing the arguments t and t' from the formal integration variables t_1 and t_2 . This gives the double integral

$$\langle w(t)w(t') \rangle = \frac{2}{\tilde{\tau}} \int_{t_1=-\infty}^t \int_{t_2=-\infty}^{t'} e^{-(t-t_1+t'-t_2)/\tilde{\tau}} \langle \xi(t_1)\xi(t_2) \rangle dt_1 dt_2.$$

Notice that the operations of integration and averaging (expectation value) are exchangeable. We now consider the case $t > t'$. Setting $\langle \xi(t_1)\xi(t_2) \rangle = \delta(t_1 - t_2)$ and using the definition $\int f(t)\delta(t)dt = f(0)$ of the Dirac δ -distribution to eliminate the integral over t_1 ¹⁰ yields

$$\langle w(t)w(t') \rangle = \frac{2}{\tilde{\tau}} \int_{t_2=-\infty}^{t'} e^{(2t_2-t-t')/\tilde{\tau}} dt_2$$

¹⁰ Since $t \geq t'$ and the above integration property of the δ -distribution only applies if the integration interval includes zero (i.e., $t_1 = t_2$), we cannot use this property to eliminate the integral over t_2 .

which can be analytically solved resulting in

$$\langle w(t)w(t') \rangle = e^{-(t-t')/\tau}.$$

If $t < t'$, the derivation proceeds analogously resulting in $\langle w(t)w(t') \rangle = e^{-(t'-t)/\tau}$. Consolidating these two cases, we arrive at

$$\langle w(t)w(t') \rangle = e^{-|t-t'|/\tau}.$$

As important special case, we obtain the variance $\langle w^2(t) \rangle = 1$. Finally, when we apply the averaging operation $\langle \cdot \rangle$ to the formal solution $w(t)$ itself using the condition $\langle \xi(t) \rangle = 0$, we obtain $\langle w \rangle = 0$, i.e., the second condition (12.7). This concludes the derivation of the statistical properties of the Wiener process.

12.2 Consequences of Estimation Errors

Overestimating the gap by 10 %, i.e., by the factor 1.1 results in a *smaller* steady-state gap. With the values of the problem statement, we obtain

$$1.1s_e = s_0 + vT \quad \Rightarrow \quad s_e = \frac{s_0 + vT}{1.1} = 28.3 \text{ m}$$

instead of the “true” steady-state $s_e = 31.1$ m. When there is a constant additive acceleration component $\Delta a = 0.4 \text{ m/s}^2$, the steady-state condition reads

$$\dot{v} = \Delta a + \frac{\frac{s_e - s_0}{T} - v}{\tau} \stackrel{!}{=} 0,$$

or $s_e = s_0 + vT - \tau a_z = 30.9$ m. Notice that the surprisingly small amount of change can be tracked back to the “rigidity” of the OVM reaction caused by the small relaxation time τ .

12.3 Multi-Anticipation for the IDM

Applying the general equation (12.17) for multi-anticipative effects to the IDM gives

$$c \sum_{j=1}^{n_a} a \left(\frac{s_0 + vT}{js} \right)^2 = a \left(\frac{s_0 + vT}{s} \right)^2,$$

hence $c = 1/(\sum_{j=1}^{n_a} \frac{1}{j^2})$, i.e., Eq. (12.18). Instead of introducing c , it is obviously possible for the IDM to *renormalize* the parameters s_0 and T by multiplying them with a common factor. For this purpose, we write the left-hand side of above equation as

$$\sum_{j=1}^{n_a} a \left(\frac{\sqrt{c}s_0 + v\sqrt{c}T}{js} \right)^2,$$

so the factor \sqrt{c} of the problem statement is evident. The factor \sqrt{c} assumes values between 1 (no multi-anticipation) and $\sqrt{6}/\pi \approx 0.78$ (multi-anticipation to infinitely many leaders). This means, the numerical values of s_0 and T are reduced by no more than 22 %.

Problems of Chapter 13

13.1 Dynamic Properties of the Nagel-Schreckenberg Model

To obtain physical units, we multiply the dimensionless desired speed of the NSM with $\Delta x/\Delta t$. Thus, $v_0 = 2$ (city traffic) corresponds to 54 km/h, and $v_0 = 5$ (highways) to 135 km/h. Likewise, multiplying the dimensionless accelerations with $\Delta x/(\Delta t)^2 = 7.5 \text{ m/s}^2$ yields the physical accelerations. In the deterministic NSM, $a = 1$, so $a_{\text{phys}} = 7.5 \text{ m/s}^2$ resulting in an acceleration time of

$$\tau_{0 \rightarrow 100} = \frac{v_{\text{phys}}}{a_{\text{phys}}} = 3.7 \text{ s.}$$

In the stochastic model, the acceleration a is realized only with a probability $(1 - p)$. So, the average acceleration time increases by a factor $(1 - p)^{-1}$ to 6.2 s.

13.2 Approaching a Red Traffic Light

The driver approaches with the desired speed v_0 until the distance to the traffic light falls below the “interaction distance” $g = v_0$. Then, there are two possibilities for the deceleration process: (i) stopping in one step (if, after crossing the interaction point, the gap in the next time step is already zero), (ii) stopping in two steps $v_0 \rightarrow v_1 \rightarrow 0$ (if the gap after crossing the interaction point is $v_1 > 0$). If $v_0 = 2$, the realized decelerations are (i) -15 m/s^2 or (ii) -7.5 m/s^2 .

13.3 Fundamental Diagram of the Deterministic NSM

Without stochastic components, the steady-state speed as a function of the gap g is well-defined:

$$v_e(g) = \max(v_0, g)$$

meaning that the macroscopic fundamental diagram (in physical units) has the well-known triangular shape given by¹¹

$$Q_e(\rho) = \min \left[V_0^{\text{phys}} \rho, \frac{1}{T} \left(1 - \frac{\rho}{\rho_{\text{max}}} \right) \right].$$

The values of its three parameters are

¹¹ We drop the superscripts “phys” denoting physical quantities where no confusion is possible, i.e., for ρ and Q . We will retain the superscripts for speeds and velocities.

$$V_0^{\text{phys}} = v_0 \Delta x / \Delta t = \begin{cases} 54 \text{ km/h} & \text{cities} \\ 135 \text{ km/h} & \text{highways,} \end{cases}$$

$$T = \Delta t = 1 \text{ s}, \quad \rho_{\text{max}} = \frac{1}{\Delta x} = 133 \text{ vehicles/km.}$$

In the stochastic model ($p > 0$), the average flow $\langle Q(\rho) \rangle$ as a function of the local density is below that of the deterministic case. The fundamental diagram is no longer triangular, and also the gradients at zero and maximum density are different. In the following two problems, we will derive

$$V_0^{\text{phys}} = Q'_e(0) = (v_0 - p) \frac{\Delta x}{\Delta t}, \quad c_{\text{cong}}^{\text{phys}}(\rho_{\text{max}}) = Q'_e(\rho_{\text{max}}) = -(1 - p) \frac{\Delta x}{\Delta t}.$$

13.4 Macroscopic Desired Speed

Without interaction and after a sufficient time, the vehicle speed is either v_0 (no dawdling in the last time step), or $v_0 - 1$ (dawdling). If $v = v_0$, then the speed will be reduced in the next time step to $v_0 - 1$ with probability p . If $v = v_0 - 1$, the speed in the next time step will reach v_0 with probability $1 - p$. The situation is stationary in the stochastic sense if expectation values do not change over time, $\langle v(t+1) \rangle = \langle v(t) \rangle$. Here, this means that the probabilities for the speeds v_0 and $v_0 - 1$ do not change over time, i.e., the unconditional “probability fluxes” from v_0 to $v_0 - 1$ and from $v_0 - 1$ to v_0 balance to zero.¹² Setting up the balance for the speed state $v = v_0$ and denoting by θ the probability for this state, the probability flux $v_0 \rightarrow v_0 - 1$ away from v_0 is $-\theta p$ (probability θ times conditional probability p ; negative sign because the flux is outflowing). The “inflowing” probability flux $v_0 - 1 \rightarrow v_0$ is $(1 - \theta)(1 - p)$ (probability $1 - \theta$ times conditional probability $1 - p$). So, stationarity implies

$$\frac{d}{dt} (\text{Prob}(v = v_0)) = -\theta p + (1 - \theta)(1 - p) \stackrel{!}{=} 0 \Rightarrow \theta = 1 - p,$$

or

$$\langle v \rangle = \theta v_0 + (1 - \theta)(v_0 - 1) = v_0 - p.$$

In physical units, this means $V^{\text{phys}} = \langle v \rangle \Delta x / \Delta t$, i.e., the result displayed above in the solution to Problem 13.4.

13.5 Propagation Velocity of Downstream Jam Fronts

Assume a queue of standing vehicles where only the first vehicle has space to accelerate. This first vehicle will accelerate with probability $1 - p$ (with probability

¹² Mathematically, this balance of probability fluxes is called a *Master equation*.

p , dawdling occurs). Only if this vehicle accelerates, the next vehicle in the queue has the possibility to accelerate in the next time step, which it does, again, with probability $1 - p$. This means, the “starting wave” propagates at an average velocity $c_{\text{cong}} = -(1 - p)\Delta x/\Delta t$. For $p = 0.4$, this yields the reasonable value $c = -16.2 \text{ km/h}$.

Problems of Chapter 14

14.1 Why the Grass is Always Greener on the Other Side?

We assume two lanes with staggered regions of highly congested traffic (ρ_1, V_1) and less congested traffic ($\rho_2 < \rho_1, V_2 > V_1$) of the same length: Whenever there is highly congested traffic on lane 1, congestion is less on lane 2, and vice versa (cf. the figure in the problem statement). Since traffic in both regions is (more or less) congested and the fundamental diagram is triangular by assumption, the transitions from region 1 and 2 and from 2 to 1 remain sharp and propagate according to the shock-wave formula (8.9) at a constant velocity

$$c = \frac{Q_2 - Q_1}{\rho_2 - \rho_1} = -\frac{l}{T} = -5 \text{ m/s}.$$

The fraction of time in which drivers are stuck in the highly congested regions is obviously equal to the fraction of time spent in regions of type 1. Denoting by τ_i the time intervals τ_i to pass one region $i = 1$ or 2, we express this fraction by

$$p_{\text{slower}} = p_1 = \frac{\tau_1}{\tau_1 + \tau_2}.$$

When evaluating τ_i , it is crucial to realize that the regions propagate in the opposite direction to the vehicles, so the relative velocity $V_i + |c|$ is relevant. Assuming equal lengths L for both regions, the passage times are $\tau_i = L/(V_i + |c|)$, so

$$p_1 = \frac{\frac{L}{V_1 + |c|}}{\frac{L}{V_1 + |c|} + \frac{L}{V_2 + |c|}} = \frac{V_2 + |c|}{V_2 + V_1 + 2|c|}.$$

For example, if $V_1 = 0$ and $V_2 = 10 \text{ m/s}$, the fraction is

$$p_1 = \frac{10 + 5}{10 + 10} = \frac{3}{4},$$

i.e., drivers are stuck in the slower lane 75 % of the time—regardless which lane they choose or of whether they change lanes or not.

Alternatively, one picks out a vehicle at random. Since the less and highly congested regions have the same length, the fraction of vehicles in the highly congested region, i.e., the probability of picking one from this region, is given by

$$p_1 = \frac{\rho_1}{\rho_1 + \rho_2} = \frac{200}{200 + 200/3} = \frac{3}{4}.$$

14.2 Stop or Cruise?

We distinguish two cases: (i) Drivers can pass the traffic light at unchanged speed in the yellow phase, i.e.,

$$s < s_1 = v\tau_y.$$

(ii) When cruising, drivers would pass the traffic light in the red phase, so stopping is mandatory. In this case, drivers need a reaction time T_r to perceive the signal, make a decision, and stepping on the braking pedal. Afterwards, we assume that they brake at a constant deceleration b so as to stop just at the stopping line. This results in the *stopping distance*

$$s = vT_r + \frac{v^2}{2b}. \quad (2.9)$$

Obviously, the *worst case* for the initial distance s to the stopping line at switching time green-yellow is the threshold $s = s_1$ between (i) and (ii), i.e., cruising is just no more legal. Inserting $s = s_1$ into Eq. (2.9) and solving for b gives

$$b = \frac{v}{2(\tau_y - T_r)} = 3.47 \text{ m/s}^2.$$

This is a significant, though not critical, deceleration. It is slightly below the deceleration 3.86 m/s^2 implied by the braking distance rule “speedometer reading in km/h squared divided by 100” (Problem 11.2) but above typical comfortable decelerations of the order of 2 m/s^2 . We conclude that the legal minimum duration of yellow phases is consistent with the driver and vehicle capabilities.

14.3 Entering a Highway with Roadwork

In this situation, we can apply both the safety criterion (14.4) of the general lane-changing model or the safety criterion of the decision model (14.27) for entering a priority road. With the notations of Fig. 14.6, we obtain for a defensive driver ($b_{\text{safe}} = 0$)

$$s_f > s_{\text{safe}}(v_f, v) = s_{\text{opt}}(v_f) = v_f T = 20 \text{ m}.$$

Here, we have dropped all hats, consistent with the convention adopted in Sect. 14.5. In the “worst case”, the driver decides to merge if the vehicle on the highway is just $s_{\text{safe}} = 20 \text{ m}$ away. Now we calculate the minimum deceleration b_{min} the driver on

the main-road has to adopt to avoid a crash. Applying the kinematic braking distance $s = \Delta v^2/(2b)$ to the critical distance $s_{\text{safe}} = 20$ m, the initial speed difference $\Delta v = v_f = 20$ m/s, and the relative deceleration $b = b_{\min} + a$ (assuming that the merging vehicle accelerates at $a = 2$ m/s²), and solving for b_{\min} results in

$$b_{\min} = \frac{v_f^2}{2s} - a = 8 \text{ m/s}^2.$$

We observe that, in spite of the very conservative assumption $b_{\text{safe}} = 0$ in the decision model, the *actually* necessary deceleration of the main-road vehicle corresponds to an emergency braking maneuver. This discrepancy can be traced back to the OVM whose braking strategy is inconsistent with kinematic constraints and does not contain the speed difference although this is a crucial exogenous factor (in fact, the OVM simulation will lead to crashes in this situation). As shown in the next problem, drivers modeled by the Gipps' model or the IDM family will make a consistent decision in this situation.

14.4 An IDM Vehicle Entering a Priority Road

In this situation (Fig. 14.6 for $v_\alpha = 0$), the IDM safety criterion (14.27) reads

$$s_f > s_{\text{safe}}^{\text{IDM}}(v_f, 0) = \frac{s_0 + v_f T + \frac{v_f^2}{2\sqrt{ab}}}{\sqrt{\frac{a_{\text{free}}(v_f)}{a} + \frac{b_{\text{safe}}}{a}}},$$

or, with $s_0 = 0$, $v_f = v_0$, and $a = b = b_{\text{safe}}$ (then, the square root is equal to 1)

$$s_f > s_{\text{safe}}^{\text{IDM}} = v_f T + \frac{v_f^2}{2b_{\text{safe}}}.$$

This means, the minimum gap to allow merging corresponds to the *stopping distance* of the follower on the main-road (braking distance $v_f^2/(2b)$ plus distance $v_f T_r$ driven during the reaction time) when the desired time headway is set equal to the reaction time, $T = T_r$. Consequently, the IDM safety criterion for merging is consistent with the driver capabilities and kinematic constraints. For $T = 1$ s, $b_{\text{safe}} = 2$ m/s², and $v_0 = 50$ km/h, we obtain as safe distance for merging $s_{\text{safe}}^{\text{IDM}} = 31$ m.

Problems of Chapter 15

15.1 Characterizing the Type of Instability

The displayed traffic flow is locally stable since, after a sufficient time, each driver reverts to the steady state (he or she stops, at most, once). At the same time, the dynamics is string unstable since the amplitude of the oscillations increase from vehicle to vehicle. The string instability is convective (of the upstream type) since

there is only a single traffic wave: After a sufficiently long time, traffic flow reverts to the steady state at any fixed location.

15.2 Propagation Velocity of Traffic Waves in Microscopic Models

At first, we transform the microscopic propagation velocity given in the comoving (Lagrangian) coordinate system to a stationary coordinate system:

$$\tilde{c} = v_e + \tilde{c}_{\text{rel}} = v_e - (s_e + l)v'_e(s_e) = v_e - \frac{v'_e(s_e)}{\rho_e}.$$

Here, we used the relation $s_e + l = 1/\rho_e$. Now we express the microscopic gradient $v'_e(s)$ by the corresponding macroscopic quantity $V'_e(\rho)$. Using the identity $v_e(s) = V_e(\rho(s))$ and the micro-macro relation $\rho = 1/(s + l)$, we obtain

$$v'_e(s) = \frac{dv_e}{ds} = \frac{dV_e}{d\rho} \frac{d\rho}{ds} = -\frac{V'_e(\rho)}{(s + l)^2} = -\rho^2 V'_e(\rho). \quad (2.10)$$

Inserting this into the expression for \tilde{c} gives the final result

$$\tilde{c} = v_e - \frac{v'_e(s_e)}{\rho_e} = V_e + \rho_e V'_e(\rho_e) = \frac{d}{d\rho_e}(\rho_e V_e) = Q'_e(\rho_e).$$

15.3 Instability Limits for the Full Velocity Difference Model

Subproblem 1: The local stability criterion is satisfied if

$$\tilde{a}_v + \tilde{a}_{\Delta v} = -\frac{1}{\tau} - \gamma \leq 0 \quad \Rightarrow \quad \gamma \geq -\frac{1}{\tau} = -0.2 \text{ s}^{-1}.$$

This is true even for slightly negative values of the sensitivity γ to speed differences (although this implies accelerations in response to positive approaching rates which is no reasonable behavior). As such, it reflects the result that all reasonable (and even some unreasonable) models without explicit delays (reaction times) are locally stable.

Subproblem 2: For $v \geq v_0$, there are no interactions and, therefore, no instabilities. If $v < v_0$, we have $v'_e(s) = 1/T$, $\tilde{a}_v = -1/\tau$, and $\tilde{a}_{\Delta v} = -\gamma$. Inserting these relations into condition (15.25) for an oscillation-free local car-following characteristics yields

$$\frac{1}{T} \leq \frac{1}{4\tau} (1 + \gamma\tau)^2.$$

Solving this quadratic inequality for γ results in

$$\gamma \geq -\frac{1}{\tau} \pm \frac{2}{\sqrt{T\tau}} = 0.69 \text{ s}^{-1}.$$

Here, we used the general plausibility condition $\gamma \geq 0$ to select the positive sign of the square root when calculating the numerical value.

Subproblem 3: To determine the limits of string instability, we use criterion (15.69). Solving the resulting inequality for γ yields

$$\gamma > \frac{1}{T} - \frac{1}{2\tau} = 0.9 \text{ s}^{-1}.$$

We observe that car-following schemes may be string unstable even if they do not produce *any* kind of oscillations (damped or otherwise) when following a single leader. Here, this applies to the parameter range $0.69 \text{ s}^{-1} < \gamma \leq 0.9 \text{ s}^{-1}$. This is highly relevant when investigating the effects of adaptive cruise control systems on traffic flow.

15.4 Stability Properties of the Optimal Velocity Model Compared to Payne's Model

The OVM criterion for string stability reads $v'_e(s) \leq 1/(2\tau)$, and the corresponding criterion for flow stability in Payne's model $-V'_e(\rho) \leq 1/(2\rho^2\tau)$. Using the micro-macro relation $v'_e(s) = 1/\rho_e^2 V'_e(\rho)$ already needed for Problem 15.2, we show the equivalence by direct substitution:

$$\frac{1}{2\tau} \geq v'_e(s_e) = -\rho_e^2 V'_e(\rho_e(s_e)) \Rightarrow -V'_e(\rho) \leq \frac{1}{2\rho^2\tau} \text{ q.e.d.}$$

15.5 Flow Instability in Payne's Model and in the Kerner-Konhäuser Model

Subproblem 1: We have solved the general flow stability problem for Payne's model already in Problem 15.4. For the triangular fundamental diagram as specified in the problem formulation, the gradient of the speed-density relation reads

$$V'_e(\rho) = \begin{cases} 0 & \rho \leq \rho_C, \\ -\frac{1}{\rho^2 T} & \rho > \rho_C, \end{cases}$$

with the density at capacity $\rho_C = 1/(v_0 T + l_{\text{eff}}) = 20$ vehicles/km. For free traffic ($\rho < \rho_C$) there are no interactions ($V'_e(\rho) = 0$) and therefore unconditional stability. Congested traffic flow ($\rho \geq \rho_C$) is stable if

$$\tau < \frac{T}{2}.$$

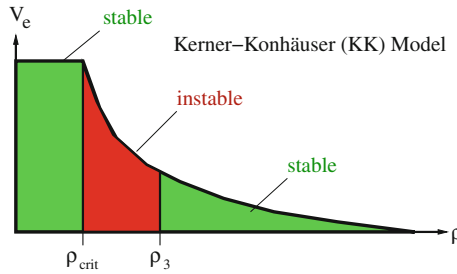
This means, Payne's model describes stable congested traffic for unrealistically small adaptation times τ , only.

Subproblem 2: For the Kerner-Konhäuser model, the flow stability criterion reads $(\rho V_e'(\rho))^2 < \theta_0$. Inserting the steady-state relation $V_e(\rho) = \max[V_0, 1/T(1/\rho - 1/\rho_{\max})]$ gives, again, unconditional stability for free traffic flow ($\rho < \rho_C = 20/\text{km}$) which is consistent with the requirements of the problem formulation. For congested traffic ($\rho > \rho_C$), we have

$$\frac{1}{\rho^2 T^2} < \theta_0.$$

From this condition, we determine θ by demanding that congested traffic flow should be unstable for densities below $\rho_3 = 50/\text{km}$, and stable above. With $T = 1.1 \text{ s}$ and $\rho_3 = 50/\text{km}$, we finally obtain (cf. the figure below)

$$\theta_0 = \frac{1}{\rho_3^2 T^2} = 331 \frac{\text{m}^2}{\text{s}^2}.$$



15.6 Flow Instability of the GKT Model

For high densities near the maximum density, we can approximate the GKT steady-state flow by $Q_e \approx 1/T(1 - \rho/\rho_{\max})$, or $V_e'(\rho) = -1/(T\rho^2) \approx -1/(T\rho_{\max})^2$. Without anticipation ($\gamma = 0$) and assuming a constant speed variance prefactor $\alpha_{\max} = \alpha(\rho) \approx \alpha(\rho_{\max})$ which is equivalent to $P_e' \approx \sigma_V^2 \approx \alpha_{\max} V_e^2$, the GKT stability criterion (15.83) becomes

$$(\rho V_e')^2 - P_e' = \frac{1}{T^2 \rho^2} - \alpha_{\max} V_e^2 \leq 0.$$

Since, for $\rho \rightarrow \rho_{\max}$, the expression $(T\rho)^{-2}$ tends to the squared propagation velocity c^2 of moving downstream jam fronts while the speed variance $\alpha_{\max} V_e^2$ tends to zero, the stability criterion cannot be satisfied: Without anticipation, the GKT model is unconditionally unstable for sufficiently high densities!

For a finite anticipation range $s_a = \gamma V_e T$, however, the third term of the stability condition (15.83) can stabilize traffic flow. Sufficiently close to the maximum density, we can approximate the full GKT flow stability criterion to an analytically tractable condition. If $\rho \approx \rho_{\max}$, we have, up to linear order in V_e

$$\rho V_e' \approx -\frac{1}{T\rho}, \quad P_e' \approx \alpha_{\max} V_e^2 \approx 0, \quad s_a(V_0 - V_e) \approx \gamma V_e V_0 T.$$

Furthermore, with $\rho_{\max}/(\rho_{\max} - \rho) \approx (\rho V_e T)^{-1}$, we can approximate the bracket of the last term of Eq. (15.83) by

$$\left[\frac{\rho_{\max}}{\rho_{\max} - \rho} - \frac{\rho V_e'}{\sigma_V \sqrt{\pi}} \right] \approx \frac{1}{\rho V_e T} \left(1 + \frac{1}{\sqrt{\alpha_{\max}}} \right).$$

Inserting all this into the GKT stability condition (15.83), we find that the GKT model is string stable for densities near the maximum density if the anticipation factor γ fulfils

$$\gamma > \frac{\tau}{2T^2 \rho_{\max} V_0 [1 + (\alpha_{\max} \pi)^{-1/2}]}$$

which is condition (15.84).

15.7 IDM Stability Class Diagram for other Parameter Values

In the following, we will denote the scaled dimensionless quantities with a tilde. According to the problem formulation, the scaled time and space coordinates as well as derived variables (speed, acceleration) are related to the unscaled quantities as

$$t = \sqrt{\frac{s_0}{b}} \tilde{t}, \quad x = s_0 \tilde{x}, \quad v = \sqrt{b s_0} \tilde{v}, \quad \frac{dv}{dt} = b \frac{d\tilde{v}}{d\tilde{t}}.$$

Inserting this transformation into the IDM equations results in

$$\begin{aligned} \frac{d\tilde{v}}{d\tilde{t}} &= \frac{a}{b} \left[1 - \left(\frac{\sqrt{b s_0} \tilde{v}}{v_0} \right)^4 - \left(\frac{\tilde{s}^*}{\tilde{s}} \right)^2 \right], \\ \tilde{s}^* &= \frac{s^*}{s_0} = 1 + \sqrt{\frac{b}{s_0}} T \tilde{v} - \sqrt{\frac{b}{a}} \frac{\tilde{v} \Delta \tilde{v}}{2}. \end{aligned}$$

As a consequence, the prefactors of the different new terms are dimensionless as well. Moreover, they come in only three combinations of the original IDM parameters which we can identify as the new model parameters:

$$\tilde{v}_0 = \frac{v_0}{\sqrt{b s_0}}, \quad \tilde{a} = \frac{a}{b}, \quad \tilde{T} = T \sqrt{\frac{b}{s_0}}.$$

Thus, the scaled IDM equations read

$$\frac{d\tilde{v}}{d\tilde{t}} = \tilde{a} \left[1 - \left(\frac{\tilde{v}}{\tilde{v}_0} \right)^4 - \left(\frac{\tilde{s}^*}{\tilde{s}} \right)^2 \right], \quad \tilde{s}^* = 1 + \tilde{v} \tilde{T} - \frac{\tilde{v} \Delta \tilde{v}}{2\sqrt{\tilde{a}}}.$$

This allows a powerful conclusion¹³: Changing the five physical IDM parameters such that \tilde{v}_0 , \tilde{a} , and \tilde{T} remain unchanged does not change the scaled IDM equations, nor the local dynamics. This allows to reduce the five-dimensional IDM parameter space spanned by V_0 , T , a , b , and s_0 to the three-dimensional space $(\tilde{V}_0, \tilde{T}, \tilde{a})$ spanned by the dimensionless parameters. However, the stability class depends not only on the local dynamics but also on the vehicle length influencing the macroscopic fundamental diagram $Q_e(\rho)$ and the sign of propagation velocities. Therefore, to ensure the same stability class, a forth dimensionless parameter

$$\tilde{l} = l/s_0$$

must be kept constant.

When applying these insights to the concrete problem of where to read off the stability class in the a - T -class diagram when other IDM parameters are changed, we observe that this is only possible if speed is changed proportionally to changes of $\sqrt{bs_0}$ and the vehicle length changes proportionally to s_0 . Only then, the two scaled parameters \tilde{v}_0 and \tilde{l} containing neither a nor T remain unchanged. This is fulfilled here since s_0 does not change anyway and the new values $v_0^* = 139$ km/h and $b^* = 2$ m/s² of the desired speed and time headway, respectively, satisfy $\tilde{v}_0 = v_0(bs_0)^{-1/2} = v_0^*(b^*s_0)^{-1/2} = \text{const.}$ In order to make sure that \tilde{a} and \tilde{T} remain unchanged as well, we read off the old diagram at the coordinate $(T^*, a^*) = (\tau T, \alpha a)$ rather than at (T, a) . We fix the scaling factors τ and α to fulfill the conditions

$$\frac{a}{b} = \frac{a^*}{b^*} = \frac{\alpha a}{b^*}, \quad T\sqrt{\frac{b}{s_0}} = T^*\sqrt{\frac{b^*}{s_0}} = \tau T\sqrt{\frac{b^*}{s_0}}$$

resulting in

$$\tau = \sqrt{\frac{b}{b^*}} = 0.87, \quad \alpha = \frac{b^*}{b} = 1.33.$$

This means, for the new values of v_0 and b , one reads of the class diagram at 0.87 times the original T coordinate and 1.33 times the original a coordinate.

15.8 Fundamental Diagram with Hysteresis

Subproblem 1: Maximum free-traffic flow:

$$Q_{\max}^{\text{free}} = v_0 \rho_{\max}^{\text{free}} = 2,400 \text{ vehicles/h.}$$

¹³ In hydrodynamics, such scale relations are the basis to measure the hydrodynamics of big objects (ships, planes etc.) by observing a scaled-down (physical) model of the object in a wind or water channel rather than observing/measuring the real thing.

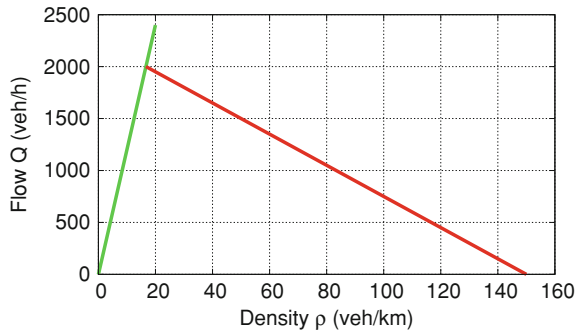
Subproblem 2: The congested part of the fundamental diagram corresponds to the congested part of the triangular fundamental diagram for the parameters $Q_{\text{cong}}(\rho) = 1/T(1 - \rho l_{\text{eff}})$ where $l_{\text{eff}} = l + s_0 = 6.67$ m. This congested branch intersects the free branch at the same point $(\rho_C, Q_{\text{max}}^{\text{dyn}})$ that would correspond to the maximum of the triangular diagram without hysteresis:

$$\rho_{\text{min}}^{\text{cong}} = \rho_C = \frac{1}{v_0 T + l_{\text{eff}}} = 16.67 \text{ vehicles/km.}$$

Subproblems 3 and 4: The jam outflow is characterized by the dynamic capacity $Q_{\text{max}}^{\text{dyn}} = v_0 \rho_C = 2,000$ vehicles/h. This describes a *capacity drop* of

$$\Delta Q = Q_{\text{max}}^{\text{free}} - Q_{\text{max}}^{\text{dyn}} = 400 \text{ vehicles/h (or 16.7 \%)}.$$

The density of the outflow is given by ρ_C . This means, hysteretic effects can take place in the density range $\rho \in [\rho_C, \rho_{\text{max}}^{\text{free}}]$, or, numerically, $\rho \in [16.67 \text{ vehicles/h, } 20 \text{ vehicles/h}]$.



Problems of Chapter 16

16.1 Influence of Serial Correlations on Measures of Parsimony

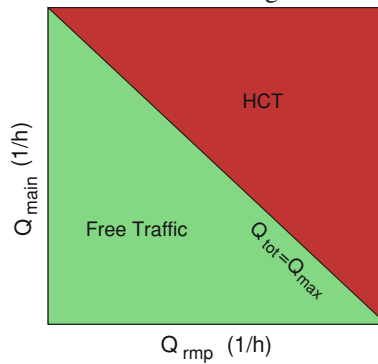
Given are twenty data points (s_i, v_i) of which the first 10 and the second 10 are identical. This means, Model (i) can fit, at least, ten data points exactly, while Model (ii) fits the data to 100%, after calibration. In contrast, if the data were not serially correlated, Models (i) and (ii) will fit at least one and two data points, respectively. This result does not depend on the specific model, since the same would apply to, say, the models (i): $\hat{v}(s) = \ln(\beta_0/s)$ and (ii): $\hat{v}(s) = \ln(\beta_0/s + \beta_1)$. This means, even completely nonsensical models fit one additional data point per parameter if the data points are independent, but they fit ten additional points if they are serially

correlated as in this example. Now assume a nonsensical addition to a given model introducing one new parameter. For iid errors in the data, a parsimony test such as the likelihood-ratio test would yield a negative result for the augmented model since each parameter can always fit one additional data point without increasing its predictive value which such tests take care of. However, for correlated data as above, this parameter explains ten additional points. For robustness tests assuming iid errors, this corresponds to nine nontrivial fits which such tests may erroneously interpret as worth the additional parameter.

Problems of Chapter 17

17.1 Phase Diagram for Stability Class 3

For class 3, there are no traffic-flow instabilities and no hysteresis. Therefore, one just distinguishes between free traffic and homogeneous congested traffic:

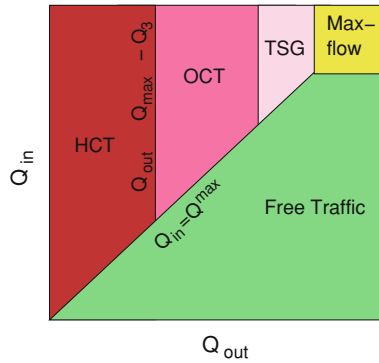


Furthermore, since no instability also implies no hysteresis effects, there is only one phase diagram valid for both small and large initial perturbations.

17.2 Boundary-Induced Phase Diagram

The kind of extended congested pattern (TSG, OCT, HCT) is directly defined by the supply restriction Q_{out} . Because of the oscillatory nature of the congested states for comparatively high values of Q_{out} (OCT and TSG), significant perturbations arrive at the upstream boundary activating the “inflow-bottleneck” if $Q_{\text{in}} > C_{\text{dyn}}$ (remember that we have $I = 1$ lane). If, additionally, $Q_{\text{out}} \geq C_{\text{dyn}}$, the potential outflow is higher than the inflow restricted by the activated inflow-bottleneck. This means there is free traffic in the bulk of the investigated road section corresponding to the maximum-flow state. If, however, $Q_{\text{out}} < C_{\text{dyn}}$, congested traffic will arise everywhere and the inflow-bottleneck (whether activated or not) is no longer relevant. Therefore, the

maximum-flow state requires both $Q_{\text{in}} > C_{\text{dyn}}$ and $Q_{\text{out}} \geq C_{\text{dyn}}$. This results in following boundary-induced phase diagram:



The situation with an activated inflow bottleneck corresponds to the stationary front of a bottleneck in inhomogeneous systems. However, since no upstream region is simulated here, the stationary front appears as a “standing wave”. In simulations, activated inflow bottlenecks are a serious problem since they introduce bottlenecks not corresponding to anything in reality. Dedicated and very complex upstream boundary conditions (not discussed here) are necessary to avoid them.

Problems of Chapter 18

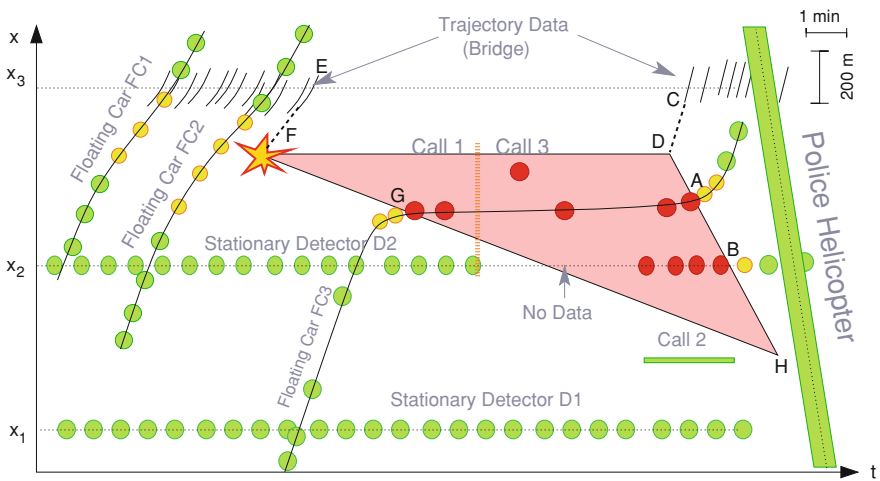
18.1 Locating a Temporary Bottleneck

From the data of floating car 3, we know that this car leaves a jam, i.e., crosses its downstream boundary, at the spatiotemporal point A depicted in the diagram below. From the data of detector 2 (point B), we know that this front is moving. We can exclude that the transition from congested to free traffic recorded by detector 2 at point B corresponds to a downstream moving upstream front because (i) detector D1 records essentially constant traffic flow, (ii) the data of the detector D2 and the floating car 3 imply an upstream propagating upstream jam front, i.e., a growing jam. Hence, the upstream front is propagating backwards as long as it exists.

From Stylized Fact 2 we know that downstream fronts are either stationary or move at a constant velocity c_{cong} . Hence, the set of possible spatiotemporal points indicating when and where the road closure is lifted, lies on a line connecting the points A and B at a position $x > x_A$. The end of the road block not only sets the downstream jam front into motion but also leads to a transition empty road \rightarrow maximum-flow state. The shockwave formula (8.9) implies that this front propagates with the desired free-flow speed v_0 . Microscopically, this transition is given by the first car passing

the accident site. This car is recorded as first trajectory of the trajectory data from the bridge at point C. Assuming, for simplicity, an instantaneous acceleration to the speed v_0 , another set of possible spatiotemporal points for the removal of the road block is given by a line parallel to the first trajectory and touching it at point C (dashed line in the diagram). Intersecting the lines \overline{AB} and the line parallel to the trajectories and going through C gives us the location and time of the lifting of the road block by the intersecting set of the two lines (point D), and also the location of the accident.

To estimate the time when the accident occurred, we determine the intersection F of the line $x = x_D$ of the temporary bottleneck, and the line representing the extrapolation of the last trajectory (point E) to locations further upstream (dashed line). Finally, because of the constant inflow recorded by D1, we know from the shockwave formula that the upstream jam front propagates essentially at a constant velocity, i.e., it is given by the line intersecting F and G. The jam dissolves when the upstream and downstream fronts meet at point H.



Problems of Chapter 19

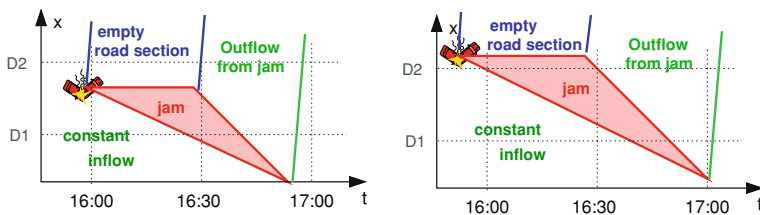
19.1 Criteria for Estimating Travel Times by N-Curves

This method works exactly on roads with a single lane per driving direction and without ramps or other non-flow-conserving bottlenecks. Without floating cars, initialization and corrections of the cumulated vehicle numbers are possible on a heuristic basis, only. If the past speed data indicate free-flow speed and there are no fast-growing differences $N_i - N_j$ between the N-curves of the detectors i and j , one assumes that there is free traffic in between, and initializes/corrects the N-curves by Eq. (19.10) with the density estimated by the average flow divided by the aver-

age speed. During the evolution of a jam (indicated by fast growing differences $N_i - N_{i+1}$), there are no correction possibilities without floating cars.

19.2 Estimating Travel Times from Aggregated Detector Data

Subproblem 1: The following figure displays two possibilities leading to the observed zero traffic flow at detector D2 between 16:00 and 16:30 h: (1) The accident happens upstream of D2 causing a temporarily empty road ($\rho = 0$, $Q = 0$) near the detector location D2. (2) The accident happens downstream of D2 causing temporarily blocked traffic ($\rho = \rho_{\max}$, $Q = 0$) near the detector location D2.



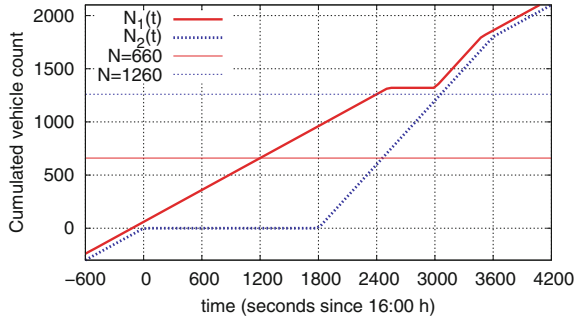
Subproblem 2: Assuming a free-flow speed of 120 km/h, it takes $\tau_{12} = 2 \text{ min} = 120 \text{ s}$ to pass the 4 km long section between the detectors D1 and D2. In this time interval, $\Delta n = 60$ vehicles have passed D1. Setting the cumulated vehicle count $N_1(0) = 0$ for the time 16:00 h (corresponding to $t = 0$), we obtain $N_2(0) = 60$. With this initialization, we calculate the cumulated vehicle count as a function of time, i.e., the N-curves, $N_1(t)$ and $N_2(t)$, by piecewise integration of the flows given in the problem statement:

$$N_1(t) = \begin{cases} 60 + 0.5 t & t < 2520, \\ 1320 & 2520 \leq t < 3000, \\ 1320 + (t - 3000) = t - 1680 & 3000 \leq t < 3480, \\ 1800 + 0.5 (t - 3480) = 60 + 0.5 t & t \geq 3480, \end{cases}$$

and

$$N_2(t) = \begin{cases} 0.5 t & t < 0, \\ 0 & 0 \leq t < 1800, \\ t - 1800 & 1800 \leq t < 3600, \\ 0.5 t & t \geq 3600. \end{cases}$$

Subproblem 3: Sketch of the N-curves:



The realized travel time $\tau_{12}(t)$ at time $t = 2,400$ s can be read from the diagram by the length of the horizontal line at height $N = N_2(2400) = 600$ s intersecting the curves $N_1(t)$ and $N_2(t)$: $\tau_{12}(t = 2,400) \approx 1,300$ s (exactly: 1,260, see below). The expected travel time $\tilde{\tau}_{12}(t)$ at time $t = 2,400$ s is equal to the length of the horizontal line at height $N_1(2400) = 1,250$ intersecting the two N-curves: $\tilde{\tau}_{12}(t) \approx 600$ s (exactly: 660).

Subproblem 4: The diagram of the N-curves shows that, when estimating $\tilde{\tau}_{12}(t)$ within the time interval $-120 \text{ s} \leq t < 2,520 \text{ s}$, the horizontal line intersecting the N-curves has a height N between $N_1(-120) = 0$ and $N_1(2,520) = 1,320$. We determine its length between the intersections with the N-curves using the results of subproblem 2:

$$N_1(t) = N_2(t + \tilde{\tau}_{12})$$

$$60 + \frac{t}{2} = (t + \tilde{\tau}_{12}) - 1,800 \Rightarrow \tilde{\tau}_{12} = 1,860 - \frac{t}{2}.$$

For $t < -120$ s, we have $\tilde{\tau}_{12} = 120$ s, i.e., equal to the free-flow travel time. At $t = -120$ s, there is a jump from 120 to 1,920, i.e., by 1,800 s or 30 min. This corresponds to the waiting time difference between the last vehicle that can pass before the road closure becomes active (possibly the car causing the accident), and the car after it having to wait the full duration of the road block.

For $\tau_{12}(t)$ within the time interval $1,800 \text{ s} \leq t < 3,120 \text{ s}$, we obtain analogously

$$N_1(t - \tau_{12}) = N_2(t)$$

$$60 + \frac{1}{2}(t - \tau_{12}) = t - 1,800 \Rightarrow \tau_{12} = 3,720 \text{ s} - t.$$

Subproblem5: Since, according to the problem statement, the floating car slows down sharply when passing D2 at 16:00h, the accident happened downstream of D2 somewhat before 16:00h. This corresponds to situation (2) discussed in subproblem 1 above.

Problems of Chapter 20

20.1 Coefficients of a Statistical Modal Consumption Model

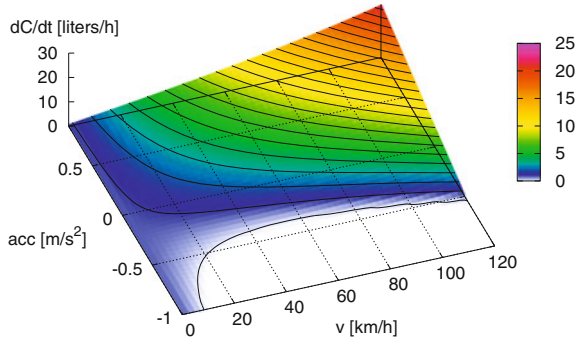
Assuming a constant specific consumption $C_{\text{spec}} = 1/(\gamma w_{\text{cal}})$ (purely analytic physics-based model) and inserting Eqs. (20.14), (20.5), and (20.4) into Eq. (20.12) gives following function for the instantaneous model consumption:

$$\begin{aligned}\dot{C} &= C_{\text{spec}} P = C_{\text{spec}} \max [0, P_0 + Fv] \\ &= C_{\text{spec}} \max \left[0, P_0 + mv\dot{v} + m(\mu + \phi)gv + \frac{1}{2}c_d\rho Av^3 \right].\end{aligned}$$

Apart from the maximum condition, this is a parameter-linear function whose parameters β_j can be easily estimated by conventional multivariate regression. Comparing this function with the statistical model specified in the problem statement and using Table 20.2 gives following relations and values for the model parameters:

$$\begin{aligned}\beta_0 &= C_{\text{spec}} P_0 &= 25.0 \cdot 10^{-3} \text{ l/s}, \\ \beta_1 &= C_{\text{spec}} mg\mu &= 24.5 \cdot 10^{-6} \text{ l/m}, \\ \beta_2 & &= 0, \\ \beta_3 &= \frac{1}{2} C_{\text{spec}} c_d \rho A &= 32.5 \cdot 10^{-9} \text{ l s}^2/\text{m}^3, \\ \beta_4 &= C_{\text{spec}} m &= 125 \cdot 10^{-6} \text{ l s}^2/\text{m}^2, \\ \beta_5 &= C_{\text{spec}} mg &= 1.23 \cdot 10^{-3} \text{ l/s}.\end{aligned}$$

The following figure gives a plot of this function:



20.2 An Acceleration Model for Trucks

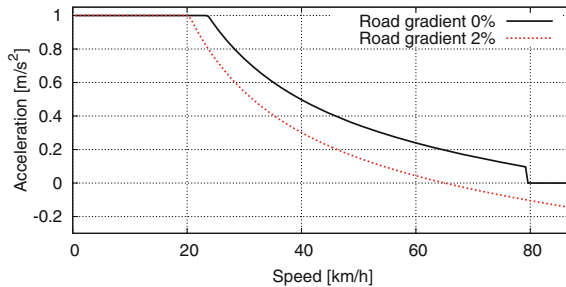
To solve this problem, we only need the power module of the physics-based modal consumption/emissions model. Assuming a constant engine power P and solving Eq. (20.5) for the acceleration gives

$$\dot{v}_P(v, \phi) = \frac{P - P_0}{mv} - g(\mu + \phi) - \frac{1}{2} c_d \rho A v^2.$$

To include the restraints “maximum acceleration a_{\max} ” and “no positive acceleration at speed $v > v_0$ ”, we obtain the final form of the free-flow truck acceleration model:

$$\dot{v}(v, \phi) = \begin{cases} \min(a_{\max}, \dot{v}_P(v, \phi)) & v \leq v_0 \\ \min(0, \dot{v}_P(v, \phi)) & v > v_0. \end{cases}$$

Following plot shows that the engine power is not sufficient to drive the truck at 80 km/h along a 2 % uphill gradient:



20.3 Characteristic Map of Engine Speed and Power

“Full throttle” corresponds to the top part of the allowed operating region for a given engine speed, i.e., to the top contourline. At 3,000 rpm it corresponds to 70 kW. For

a power demand of 60 kW, an engine speed $f = 3,300$ rpm (or the speed nearest to this value allowed by the transmission) results in most efficient fuel usage.

20.4 Characteristic Map of Engine Speed and Mean Effective Pressure

(i) 60 kW, (ii) An engine speed of $2,600 \text{ min}^{-1}$ results in a specific consumption below 375 ml/kWh while, at $4,000 \text{ min}^{-1}$, the specific consumption is above 400 ml/kWh. The first option is more efficient.

20.5 Does Jam Avoidance Save Fuel? At high vehicle speeds, the aerodynamic drag becomes dominant and the consumption per kilometer increases nearly quadratically. Therefore, the savings potential decreases and can even become negative (when comparing homogeneously flowing congested traffic with high-speed free traffic).

20.6 Influencing Factors of Fuel Consumption Combining Eqs. (20.16), (20.14), (20.5), and (20.4) for the purely analytical physics-based model (constant specific consumption), we obtain following relation for the consumption per travel distance:

$$C_x = \frac{dC}{dx} = C_{\text{spec}} \max \left[0, \left(\frac{P_0}{v} + m\dot{v} + (\mu + \phi)mg + \frac{1}{2}c_d\rho Av^2 \right) \right]. \quad (2.11)$$

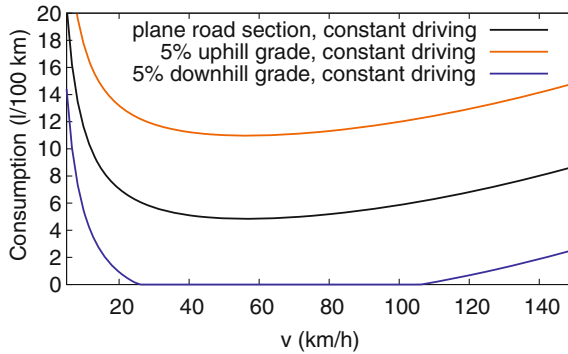
1. *Air condition*: Correct. The additional power ΔP_0 results in an additional consumption $\Delta C_x = C_{\text{spec}} \Delta P_0 / v$ which increases for decreasing speed. (Numerical values for $\Delta P_0 = 4$ kW: 3 l/100 km at 40 km/h and 1.5 l/100 km at 80 km/h.)

2. *Roof rack*: False. It is true that the increased c_d value increases the consumption per distance by $\Delta C_x = C_{\text{spec}} \Delta c_d \rho A v^2 / 2$. However, this increase grows *quadratically* with the vehicle speed, i.e., it is lowest for city traffic. (Numerical values for $\Delta c_d = 0.08$: 0.43 l/100 km at 80 km/h and 1.71 l/100 km at 160 km/h)

3. *Disconnecting the clutch when driving downhill*: False. If the clutch is disconnected, the driving shaft is decoupled from the generator and the overrun fuel cut-off cannot operate. In this case, the instantaneous consumption rate is given by the idling consumption rate $\dot{C}_0 = C_{\text{spec}} P_0$ leading to $C_{x0} = C_{\text{spec}} P_0 / v$ for the consumption per distance. With the clutch connected, the fuel consumption C_x is less than C_{x0} if $F < 0$, and the overrun fuel cut-off is fully operative, i.e., $C_x = 0$, if $F < -P_0 / v$. (Numerical values at 50 km/h: $C_{x0} = 1.81$ l/100 km; downhill gradient where the driving resistance F is equal to zero: -2.5% ; downhill gradient where the overrun fuel cut-off is fully operative: -4.0% .)

4. *Only use half the capacity of the tank*: False. At a tank capacity of 60 l, the average fuel volume is 30 l for the cycle full-empty-full etc, and 15 l for the cycle half filled-empty-half-filled etc. This corresponds, on average, to a savings of the total mass by $\Delta m < 15$ kg (since the specific mass of fuels is less than 1 kg/l). The resulting effect on the consumption per distance, $\Delta C_x = -C_{\text{spec}} \Delta m g \mu < 0.025$ l/100 km, is independent of the speed v and negligible (but the risk to run out of fuel increases).

5. *Reduce speed from 50 to 30 km/h:* False. At speeds below the optimal value of about 50–60 km/h (cf. the figure below), the consumption (2.11) per distance increases with decreasing speed. Specifically, $C_x = 5.7$ l/100 km at 30 km/h and 4.9 l/100 km at 50 km/h.



6. *Reduce speed from 150 to 130 km/h:* Correct. $C_x = 7.4$ l/100 km at 130 km/h and 8.7 l/100 km at 150 km/h (cf. the figure above).

20.7 Highway Versus Mountain Pass: Which Route needs More Fuel? When choosing alternative 1, i.e., driving the level highway at 150 km/h, one needs 8.7 l/100 km (cf. Solution to Problem 20.6).

When choosing alternative 2, i.e., driving the mountain pass at 72 km/h, one needs fuel only for the 50 % of the route going uphill while the downhill gradient of 8 % is more than enough to fully activate the overrun fuel cut-off (cf. the figure at the solution to Problem 20.6). With Eq. (2.11), we obtain for the uphill sections ($\phi = 0.08$) a consumption $C_x = 14.8$ l/100 km. For the complete mountain pass (uphill and downhill), the consumption halves to $C_x = 7.4$ l/100 km which is less than the consumption on the highway! (The balance tips over to the other side for gradients of more than 10 % or when driving more slowly on the highway.)

20.8 Four-way-stops Versus Intersection with Priority Rules

The analysis of situation II (constant speed $v_0 = 16$ m/s) is easy: With Eq. (2.11), we obtain for the 500 m long stretch between two intersections

$$C_{II} = LC_x = 24.2 \text{ ml.}$$

For situation I, we separate the driving cycle between two intersections into three driving modes: (i) accelerating from zero to v_0 , (ii) cruising at v_0 , and (iii) decelerating to a full stop at the next intersection.

(i) *Acceleration phase.* With $\dot{v} = a = 2 \text{ m/s}^2$, this phase lasts a time interval of $t_a = 8$ s during which a distance of $L_a = v_0^2/2a = 64$ m is covered. Because both C_x and \dot{C} are variable during the acceleration phase, explicit integration is necessary. We choose integration over time. With Eq. (20.12) and $C_{\text{spec}} = 1/(\gamma w_{\text{cal}})$, the integrand \dot{C} reads

$$\dot{C}(t) = \frac{dC}{dt} = C_{\text{spec}} \left(P_0 + m\dot{v}v(t) + (\mu + \phi)mgv(t) + \frac{1}{2}c_d\rho Av^3(t) \right). \quad (2.12)$$

With $v(t) = at$, the integration can be evaluated analytically:

$$\begin{aligned} C_{\text{acc}} &= \int_0^{t_a} \dot{C}(t) dt \\ &= C_{\text{spec}} \int_0^{t_a} \left(P_0 + ma^2t + \mu mgat + \frac{1}{2}c_d\rho Aa^3t^3 \right) dt \\ &= C_{\text{spec}} \left(P_0 t_a + \frac{1}{2}ma(a + \mu g)t_a^2 + \frac{1}{8}c_d\rho Aa^3t_a^4 \right). \end{aligned}$$

Using $t_a = v_0/a$ and $L_a = \frac{1}{2}at_a^2$, we simplify this expression to

$$C_{\text{acc}} = C_{\text{spec}} W_{\text{acc}} = C_{\text{spec}} \left(P_0 t_a + \frac{1}{2}mv_0^2 + m\mu gL_a + \frac{1}{4}c_d\rho Av_0^2 L_a \right) = 19.8 \text{ ml}.$$

The terms in the parenthesis of the last equation have the following meanings: $P_0 t_a$ is the energy necessary to operate all the secondary appliances during the acceleration phase, $\frac{1}{2}mv_0^2$ is the kinetic energy at the end of this phase, $m\mu gL_a$ is the energy lost (or, more precisely, transformed to heat) by the solid-state friction, and $\frac{1}{4}c_d\rho Av_0^2 L_a$ is the energy lost by the aerodynamic drag.

(ii) *Cruising phase.* Since both the acceleration and deceleration phases cover a road section of $L_a = 64$ m, a distance $L_c = L - 2L_a = 372$ m remains for the cruising phase. Correspondingly,

$$C_{\text{cruise}} = C_{\text{spec}} W_{\text{cruise}} = L_c C_x(v_0, \dot{v} = 0) = 18.0 \text{ ml}.$$

(iii) *Deceleration phase.* Due to overrun fuel cutoff, no fuel is consumed in this phase, so $C_{\text{brake}} = 0$.¹⁴

Result for situation I: The total consumption between two intersections for the traffic rules of situation I equals

$$C_I = C_{\text{acc}} + C_{\text{cruise}} + C_{\text{brake}} = 37.9 \text{ ml}$$

which has to be compared with $C_{II} = 24.2$ ml.

¹⁴ Strictly speaking, this is not true for the very last part of the deceleration phase when the speed (ignoring aerodynamic drag) drops below $v_c = P_0/[m(|\dot{v}| - \mu g)] \approx 7$ km/h. This is neglected here.

In summary, the fuel saving potential of changing the traffic rules from that of situation I to that of situation II is about 35 % which is massive.

20.9 Under Which Conditions Do All-Electric Cars Save CO₂ emissions?

The gasoline vehicle is treated as in Problem 20.8 with an increased cruising speed for situation II: Per kilometer, i.e., doubling the values between two intersections, we obtain following fuel consumptions for situations I and II:

$$C_x^I = 0.076 \text{ l/km}, \quad C_x^{II} = 0.074 \text{ l/km},$$

or, with 2.39 kg CO₂/l, the CO₂ emissions

$$E_x^{I, \text{gas}} = 181 \text{ g/km}, \quad E_x^{II, \text{gas}} = 176 \text{ g/km}.$$

For the all-electric car in situation I, we need per kilometer (i.e., for two start-stop cycles between intersections) a total electrical energy of

$$W_{\text{el}}^I = 2 \left[\frac{1}{\gamma_{\text{el}}} (W_{\text{acc}} + W_{\text{cruise}} + \gamma_{\text{rec}} W_{\text{brake}}) \right] = 794 \cdot 10^3 \text{ Ws}$$

where the required mechanical work for the acceleration and cruising phases of the driving cycle between two intersections is calculated as in Problem 20.8, and the mechanical work for the braking phase is that of the acceleration phase minus the double kinetic energy at cruising speed, $W_{\text{brake}} = W_{\text{acc}} - mv_0^2$:

$$W_{\text{acc}} = 238 \cdot 10^3 \text{ Ws}, \quad W_{\text{cruise}} = 216 \cdot 10^3 \text{ Ws}, \quad W_{\text{brake}} = -146 \cdot 10^3 \text{ Ws}.$$

The required total electrical energy per kilometer in situation II (cruising at 130 km/h) is calculated from the mechanical energy “power times time”,

$$W_{\text{el}}^{II} = \frac{1}{\gamma_{\text{el}}} \frac{P}{v} 1 \text{ km} = 1042 \cdot 10^3 \text{ Ws}.$$

With an energy mix of 600 g CO₂ per kWh electrical energy, the global CO₂ emissions due to operating the electric car in the two situations amounts to

$$E_x^{I, \text{el}} = 132 \text{ g/km}, \quad E_x^{II, \text{el}} = 174 \text{ g/km}.$$

Comparing this with the emissions of the gasoline car, we conclude that the all-electrical car emits significantly less CO₂ in city traffic but the global CO₂ emissions differ insignificantly when driving on highways. Of course, the results depend on many assumptions. For example, the battery adds about 150 kg to the electric vehicle (which is neglected here), the energy mix in Europe is more favorable, etc. However,

these assumptions are all transparent in the physics-based consumption/emission models.

20.10 Fuel Consumption for an OVM-Generated Speed Profile

Subproblem 1: The OVM free acceleration $\dot{v} = (v_0 - v)/\tau$ is maximal at $v = 0$. Prescribing $\dot{v}_{\max} = v_0/\tau = 2 \text{ m/s}^2$ gives the relaxation time $\tau = v_0/a = 16.67 \text{ s}$.¹⁵

Subproblem 2: We calculate the instantaneous power at a given speed v from Eq. (20.5) with Eq. (20.4):

$$P(v, \dot{v}) = \frac{\dot{C}(v, \dot{v})}{C_{\text{spec}}} = P_0 + m\dot{v}v + (\mu + \phi)mgv + \frac{1}{2}c_d\rho Av^3.$$

Inserting the OVM free acceleration $\dot{v} = (v_0 - v)/\tau$, we obtain $P_{\text{OVM}}(v) = A_0 + A_1v + A_2v^2 + A_3v^3$ where

$$\begin{aligned} A_0 &= P_{0m} = 3 \text{ kW}, & A_1 &= \eta \left(g\mu + \frac{v_0}{\tau} \right) = 3,294 \text{ W s/m}, \\ A_2 &= -\frac{\tau}{2} = -90 \text{ W (s/m)}^2, & A_3 &= \frac{1}{2}c_d\rho A = 0.39 \text{ W (s/m)}^3. \end{aligned}$$

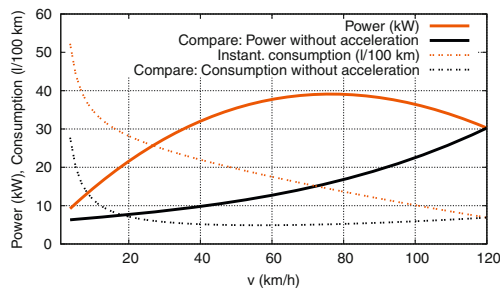
Subproblem 3: As usual, we calculate extremal values by setting the derivative with respect to the interesting variable (here, the speed v) equal to zero:

$$\frac{dP_a}{dv} = A_1 + 2A_2v + 3A_3v^2 \stackrel{!}{=} 0.$$

This quadratic equation has two solutions and corresponding extremal power requirements P_{OVM} :

$$\begin{aligned} v_1 &= 132.6 \text{ m/s} = 477.4 \text{ km/h}, & P_{\text{OVM}}(v_1^*) &= -233 \text{ kW}, \\ v_2 &= 21.2 \text{ m/s} = 76.4 \text{ km/h}, & P_{\text{OVM}}(v_2^*) &= 36.1 \text{ kW}. \end{aligned}$$

Obviously, the second solution is the correct one since the power (and the OVM acceleration) is negative for the first one.¹⁶ The maximum power during the acceleration phase is reached at 76 km/h. Its value is 36.1 kW.



20.11 Trucks at Uphill Gradients

¹⁵ At this value, the OVM is extremely unstable and cannot be used for simulating interacting or congested traffic.

¹⁶ This solution represents the minimum power requirement.

1. *Engine power:* With Eqs. (20.5) and (20.4), we obtain for the necessary power to maintain a speed $v = v_{\text{limit}} = 80 \text{ km/h}$ at level roads

$$P_{\text{dyn}} = P - P_0 = vF(v) = \mu mgv + \frac{1}{2}c_d\rho Av^3 = 249 \text{ kW} + 57 \text{ kW} = 306 \text{ kW}.$$

2. *Initial deceleration:* The two new forces entering the balance are the uphill-slope force and the inertial force. Since, initially, all other forces remain unchanged, the two new forces must cancel each other, i.e.,

$$\phi g + \dot{v} = 0 \Rightarrow \dot{v} = -\phi g = \begin{cases} -0.49 \text{ m/s}^2 & \text{at 5 \% gradient,} \\ -0.39 \text{ m/s}^2 & \text{at 4 \% gradient.} \end{cases}$$

3. *Terminal speed:* Equation (20.5) also delivers the terminal speed at a gradient ϕ by setting $\dot{v} = 0$ and solving for v . Neglecting the aerodynamic drag, we obtain

$$P_{\text{dyn}} = (\mu + \phi)gm v \Rightarrow v_{\infty} = \frac{P_{\text{dyn}}}{(\mu + \phi)gm} = \begin{cases} 10.2 \text{ m/s} & \text{at 5 \% gradient,} \\ 11.7 \text{ m/s} & \text{at 4 \% gradient.} \end{cases}$$

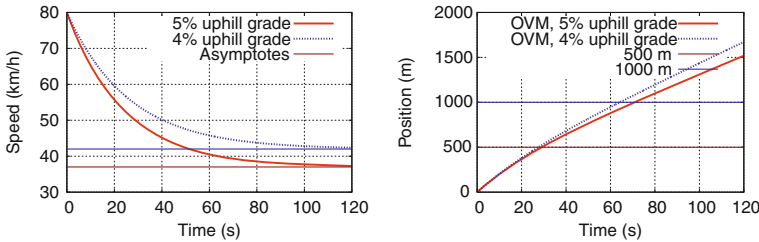
4. *Estimating the OVM parameters in the uphill section:* Since the OVM speed approaches asymptotically the desired speed v_{∞} , we can set the OVM “desired speed” in the uphill sections equal to the terminal speed v_{∞} . The initial accelerations calculated in subproblem 2 at the desired speed v_0 of the *level* section serve to estimate τ via $\dot{v} = (v_{\infty} - v_0)/\tau$, i.e., $\tau = (v_{\infty} - v_0)/\dot{v}$, resulting in

$$\tau = \begin{cases} 24.4 \text{ s} & \text{at 5 \% gradient,} \\ 26.8 \text{ s} & \text{at 4 \% gradient.} \end{cases}$$

5. *Speed and distance over time:* The solution to the inhomogeneous ordinary differential equation $\frac{dv}{dt} = (v_{\infty} - v)/\tau$ for the initial condition $v(0) = v_0$ reads (cf. the following figure)

$$v(t) = v_{\infty} + (v_0 - v_{\infty})e^{-t/\tau},$$

$$x(t) = v_{\infty}(t - \tau) + v_0\tau - (v_0 - v_{\infty})\tau e^{-t/\tau}.$$



For the uphill section 1 of length $L_1 = 500 \text{ m}$ and gradient $\phi_1 = 5 \%$, we obtain for the time $t = t_1 = 29.1 \text{ s}$ given in the problem statement:

$$v(t_1) = 13.8 \text{ m/s} = 49.8 \text{ km/h.}$$

(Test: $x(t_1) = 500.5 \text{ m.}$) Analogously, we obtain for the uphill section 2 of length $L_2 = 1,000 \text{ m}$ and gradient $\phi_2 = 4\%$ at time $t = t_2 = 64.2 \text{ s}$:

$$v(t_2) = 12.6 \text{ m/s} = 45.2 \text{ km/h.}$$

(Test: $x(t_2) = 1000.2 \text{ m.}$)

Discussion: Although the uphill section 1 is steeper, the speed of the trucks at its end is higher than at the end of the less steep but longer uphill section 2. Therefore, it makes sense to allow higher gradients on shorter uphill sections.

Index

A

ACC. *See* Adaptive cruise control
ACC model. *See* Adaptive Cruise Control Model
Acceleration
 free-flow, 181
 interaction, 215
Acceleration function
 conditions, 181
 macroscopic, 128
 microscopic, 159, 181
Acceleration noise. *See* Noise
Accident, 100, 170, 183, 217, 242, 259
Action point, 221
Action point model. *See* Model
Adaptation time. *See* Speed adaptation time
Adaptive cruise control, 58, 164, 190, 205, 270, 382, 412
Adaptive Cruise Control Model. *See* Model
Adaptive smoothing method, 40, 59, 355
ADAS. *See* Advanced driver assistance systems
Advanced driver-assistance systems, 58
Aerodynamic drag coefficient, 389
Aggregation, 58
Agility, 220, 278, 287, 412
All-electric vehicle, 390
Amoeba method, 306
Anticipation, 58, 130, 206, 278
 IDM, 224
 multi-vehicle, 206, 215
 spatial, 206
 temporal, 206
ASM. *See* Adaptive smoothing method
Attention span, 208
Autocorrelation, 211
Automatic start/stop system, 387

Average

arithmetic, 15
harmonic, 15
local, 37, 396

B

Bando Model. *See* Optimal Velocity Model
Baseline, 311
Bistability, 193
Boltzmann factor, 143, 449
Boomerang effect, 290
Bottleneck, 89, 99, 100, 113, 339, 356, 403
 activated, 167, 337, 355, 440
 activation, 260, 341
 behaviorally induced, 102, 354
 flow-conserving, 101, 102, 339, 354
 inflow, 351
 moving, 26
 non-flow-conserving, 100
 permanent, 356
 temporary, 89, 356
Bottleneck capacity. *See* Bottleneck strength
Bottleneck strength, 101, 104, 340, 343
 on-ramp, 104
Boundary conditions, 62, 112, 122, 418
 Dirichlet, 347
 downstream, 112
 upstream, 326, 347, 444
 Von-Neumann, 347
Braess's paradox, 404
Brake lights, 199, 218
Braking deceleration, 168, 183, 191, 217, 251
Braking distance. *See* Stopping distance
Braking distance rule
Braking strategy, 190, 251
 self-regulating, 191

B (cont.)

Breakdown. *See* Traffic breakdown
 Brownian motion, 136
 Bumper-to-bumper distance, 158, 182
 Burgers' equation, 121

C

CA. *See* Cellular automaton
 CAH. *See* Constant-acceleration heuristic
 Calibration, 43, 96, 210, 303, 333
 CAN-bus, 306
 Capacity, 31, 93
 dynamic, 262, 339, 404, 412, 413
 static, 262, 339, 412
 Capacity drop, 30, 33, 193, 219, 262, 312, 339, 356, 407
 Capacity hole, 113, 412
 Capacity restraint function, 61
 Car-following model. *See* Model
 Car-following regime, 173, 182
 Cell-transmission model. *See* Model
 Cellular automaton. *See* Model
 Central-limit theorem, 213
 CFL. *See* Courant-Friedrichs-Lévy
 Conditions
 Chaos
 deterministic, 421
 molecular, 142
 Characteristic map, 384, 392
 Characteristic velocities, 150
 Closed system. *See* System
 Coffeemeter, 417, 420
 Cole-Hopf transformation, 121
 Collective phenomena, 57
 Communication
 infrastructure-to-vehicle, 58, 413
 vehicle-to-vehicle, 58, 143
 Comoving with the vehicles, 137
 Completeness of data, 307
 Concave, 85
 Congested traffic pattern, 259, 340
 Congestion charge, 404
 Conservation law, 90, 146
 Consistency order, 149, 161
 Constant-acceleration heuristic, 198, 214
 Constant-speed heuristic, 214
 Consumption model. *See* Emission model
 Continuity equation, 67
 Lagrangian formulation, 77
 Control parameter, 294
 Convective instability. *See* Instability
 Convolution, 37
 Cooperation, 206, 240

Correlation, 19, 164, 211, 221
 serial, 305, 317
 Correlation coefficient, 19
 Coupled map. *See* Iterated map
 Courant-Friedrichs-Lévy conditions, 91, 140, 151
 Courtesy, 206
 Covariance, 19
 Crank-Nicholson method, 147
 Crankshaft, 382
 Cross-entropy method, 310
 CTM. *See* Cell-transmission model
 Cumulated vehicle number, 369
 Cycle-variable model. *See* Emission model

D

Data
 aggregated, 15
 macroscopic, 15
 Data fusion, 45
 Dawdling, 229
 Dead time, 207
 Decision time, 207
 Delay, 257
 δ -function, 221
 Demand, 25, 55, 100
 Density. *See* Traffic density
 Derivative
 convective, 75
 local, 76
 material, 75, 128
 partial, 76
 substantial, 75, 76
 total, 75, 76
 Desired direction, 63
 Desired speed. *See* Speed
 Detector
 cross-sectional, 17
 induction loop, 13
 double, 13
 single, 13
 stationary, 20, 371
 virtual, 59, 141, 167, 327
 Deterministic chaos. *See* Chaos
 Difference equation, 81
 Differential equation
 partial hyperbolic, 145
 delay, 173, 207, 270
 ordinary, 60, 159
 partial, 59, 81, 127, 128
 Diffusion, 121, 136, 151
 numerical, 91, 136, 153, 287
 Diffusion constant, 121

Dirac function. *See* δ -function
 Dirichlet conditions. *See* Boundary conditions
 Disaggregation, 58
 Discomfort, 420
 Discrete choice
 operative level, 240
 strategic level, 240
 tactical level, 240
 Discretization errors, 149
 Dispersion, 135
 numerical, 153
 Dispersion fan, 84
 Distance gap, 14, 163
 Distance headway, 14
 Distance headway field, 77
 Disutility, 420
 Diverge, 109
 Downwind finite differences, 149
 Driven particles, 162
 Driver-vehicle unit, 1, 27, 62, 157
 Driving pattern, 381
 Driving resistance, 387
 Driving simulator, 3, 58
 Dynamic capacity. *See* Capacity
 Dynamic routing, 410

E

Effective total cylinder volume, 392
 Efficiency factor, 391, 392
 Eigenvector, 275
 Einstein, Albert, 136
 Elephant race, 416
 Emission model
 area-wide, 380
 average-speed, 381
 cycle-variable, 383
 microscopic, 381
 modal, 381
 load-based, 385, 386
 phenomenological, 385
 physics-based, 385, 386
 speed-profile, 381
 traffic-situation, 381
 traffic-variable, 381
 Endogenous variable. *See* Variable
 Energy density, 390
 Engine efficiency, 387, 390
 Engine operating point, 391
 Engine speed, 382, 391, 392
 normalized, 392
 Equilibrium assumption, 81
 Estimation error, 61, 206
 gap, 210

 persistence, 211
 speed, 210
 time dependence, 211
 Euler scheme. *See* Numerical update
 Eulerian representation, 75
 Exogenous variable. *See* Variable
 Extended floating-car data.
 See Floating-car data
 Extensive quantity, 424

F

F-test, 312
 Factsheet. *See* Model
 FCD. *See* Floating-car data
 Filtering dilemma, 415
 Finite difference, 145
 Finite-size effects, 294
 First-order model. *See* Model
 First-principles model. *See* Model
 Floating-car data, 7, 8, 45, 368, 371
 Floating-phone data, 45, 368
 Flow. *See* Traffic flow
 microscopic, 15
 Flow density, 92
 Flow-density diagram, 82, 163
 microscopic, 15
 Force
 aerodynamic drag, 389
 downhill-slope, 389
 electrostatic, 215
 friction, 387
 gravitation, 215
 inertial, 388
 social, 63, 162, 215, 219
 Fourier expansion, 273
 Fourier modes, 280
 FPD. *See* Floating-phone data
 Full Velocity Difference Model. *See* Model
 Functional, 212, 418
 Fundamental diagram, 30, 82
 concave, 90
 congested branch, 93
 free branch, 93
 inverse- λ form, 262
 microscopic, 15, 163, 267
 parabolic, 437
 triangular, 91
 FVDM. *See* Full Velocity Difference Model

G

Game of Life, 225
 Gap, 14, 195

G (cont.)

- desired, 258
- distance, 9, 14
- time, 14
- Gap-acceptance rule, 246
- Gas-kinetic based traffic model. *See* Model
- Gauss-Newton algorithm
- General Motors model. *See* Model
- Genetic algorithm, 309
- Gipps' model. *See* Model
- GKT model. *See* Gas-kinetic based traffic model
- Godunov scheme, 90, 105, 149
- Gradient descent method, 309
- Greedy algorithm, 411
- Green's function, 122
- Gridlock, 108, 408, 417
- Ground truth, 43

H

- Harmonic mean, 15
- HCT. *See* Homogeneous congested traffic
- HDM. *See* Human Driver Model
- Headway, 14, 20
 - distance, 9, 14
 - time, 9, 14
- Heaviside function, 198
- Heterogeneity. *See* Traffic
- Heuristic, 214
- High-flow state, 356
- Homo oeconomicus, 241
- Homogeneous congested traffic, 344, 349
- Homogeneous synchronized traffic, 345, 349
- HOV lane, 404
- HST. *See* Homogeneous synchronized traffic
- Human Driver Model. *See* Model
- Hybrid model, 58
- Hybrid navigation, 411
- Hybrid vehicle, 390
- Hysteresis, 94, 193, 262

I

- IDM. *See* Intelligent Driver Model
- IIDM. *See* Improved Intelligent Driver Model
- Improved Intelligent Driver Model. *See* Model
- Incentive criterion, 241
 - MOBIL, 244
- Induction loop. *See* Detector
- Inflow, 70
- Information flow, 148, 150, 418
- Inhomogeneity, 99
- Initial conditions, 62, 122

Instability, 97

- absolute, 263
- collective, 261
- convective, 150, 259, 263, 346
- diffusive, 151
- flow, 259, 261, 282
- linear, 262
- local, 259
- long-wavelength, 266, 271, 276
- macroscopic, 279
- nonlinear, 152, 262
- numerical, 150, 259
- numerical convective, 150
- physical, 259
- platoon, 261
- short-wavelength, 266
- string, 261, 259, 271
 - absolute, 260
 - convective, 260

Instantaneous travel time. *See* Travel time

Intelligent Driver Model. *See* Model

Intelligent transportation systems, 4, 58, 364, 382, 404

Inter-driver variability. *See* Variability

Interaction, 41, 181, 362

Internal consistency, 317

Interpolation

- adaptive, 42
- isotropic, 39
- linear, 208
- spatiotemporal, 37, 40

Intersection, 251

Intra-driver variability. *See* Variability

Inverse- λ form, 33, 193, 262, 339

Iterated map. *See* Model

ITS. *See* Intelligent transportation systems

J

Jam front, 133

- downstream, 76, 167, 362
- upstream, 95, 167

Jerk, 168, 188, 419

K

Kalman filter, 306

Kernel-based averaging, 58

Kerner-Klenov-Wolf model. *See* Model

Kerner-Konhäuser model. *See* Model

Kinematic deceleration, 191

Kinematic waves, 83

KK model. *See* Kerner-Konhäuser model

KKW model. *See* Kerner-Klenov-Wolf model

Korteweg-de-Vries equation, 294

Krauss model. *See* Model

L

Lag gap, 245, 246

Lagrange multiplier, 49

Lagrangian coordinates, 127

Lagrangian formulation. *See* Continuity equation

Lane change

active, 198

discretionary, 244, 405

mandatory, 244

passive, 198, 315

Lane closure, 72, 240

Lane-changing model, 62, 157

decision, 239

gap-acceptance, 246

MOBIL, 245

Lane-changing rate, 10

Lateral dynamics, 62

Lead gap, 246

Least squared errors, 304

Level of service, 381

Levenberg–Marquardt algorithm, 309

Lighthill–Whitham–Richards model.

See Model

Likelihood function, 305

Likelihood ratio test, 312

Load balancing, 410

Log-likelihood, 306

Longitudinal dynamics, 62, 157

LOS. *See* Level of service

Low-pass filter, 39

LSE. *See* Least squared errors

LWR. *See* Lighthill–Whitham–Richards model

M

Macro-micro link, 97

Map-matching, 7

Markov chain, 225

Master equation, 58, 225, 470

Maximum likelihood method, 304

Maximum-flow state, 96, 351

McCormack

corrector, 147

predictor, 147

Mean effective pressure, 391

Mean flow

arithmetic, 16

Mean speed

arithmetic, 16

harmonic, 16

Mean squared errors, 304

Memory effect, 206

Mental processing time, 207

Merge, 107

Metastability, 262, 263, 295

Micro-macro link, 59, 163

Minimal model. *See* Model

Mirrored- λ form. *See* Inverse- λ form

ML method. *See* Maximum likelihood method

MLC *See* Moving localized cluster

MOBIL *See* Lane-changing model

Modal consumption characteristics, 392

Modal emission model. *See* Emission model

Mode choice, 2

Model

acceleration, 157

action point, 188, 220

adaptive cruise control, 199

calibration. *See* Calibration

car-following, 57

continuous-time, 159

discrete-time, 160

cell-transmission, 91, 145, 237, 364

cellular automaton, 57, 60, 225

complete, 157, 171

deterministic, 61

fact sheet, 164

first-order, 82, 127, 258

first-principles, 61, 158, 187

fitting power, 333

Full velocity difference, 171, 247

gas-kinetic, 58

Gas-kinetic based traffic, 142

General motors, 158

Gipps, 184

heuristic, 61, 158

Human driver, 206, 216

hydrodynamic, 57

Improved intelligent driver, 197

input, 205

Intelligent driver, 187

scaled units, 300

iterated map, 60, 70, 160

Kerner-Klenov-Wolf, 233

Kerner-Konhäuser, 140

Krauss, 187

lane-changing. *See* Lane-changing model

Lighthill–Whitham–Richards, 82

longitudinal, 157

macroscopic, 57

local, 128

multi-lane, 72

M (*cont.*)

mesoscopic, 58
 microscopic, 57
 minimal, 181
 MOBIL *See* Lane-changing model
 multi-class, 62, 405
 multinomial logit, 241
 multinomial probit, 241
 Nagel-Schreckenberg, 229
 Newell, 139, 173
 generalized, 177
 Optimal velocity, 168, 246
 parsimonious, 240
 Paveri-Fontana
 Payne, 138
 pedestrian, 63
 predictive power, 311, 333
 psycho-physiological, 206, 221
 reliability, 333
 robustness, 44, 144, 170, 185, 237, 311, 333, 367
 scope, 183
 second-order, 82, 127
 section-based, 91, 364
 social-force, 63
 stochastic, 61, 229
 sub-microscopic, 239, 297
 traffic stream, 60
 Wiedemann, 188, 221
 Model artefact, 231
 Molecular chaos. *See* Chaos
 Moving jam, 363
 Moving localized cluster, 343, 349, 361
 MovSim, 4, 408, 411
 MSE. *See* Mean squared errors
 Multi-anticipation. *See* Anticipation
 Multi-particle model, 58
 Multinomial logit model. *See* Model
 Multinomial probit model. *See* Model

N

N-curve. *See* Cumulated vehicle number
 Nagel-Schreckenberg model. *See* Model
 Navigation device, 3, 7
 connected, 411
 Network, 107
 Newell model. *See* Model
 Newton's method, 308
 Noise
 acceleration, 61, 213, 217, 221
 exogenous, 61
 parameter, 62
 Noise pollution, 406

Nonlinear optimization, 421
 Nonlinear wave equation, 83
 NSM. *See* Nagel-Schreckenberg model
 Numerical complexity, 91, 140
 Numerical diffusion, 92
 Numerical instability. *See* Instability
 Numerical integration, 145, 161
 Godunov scheme, 90
 McCormack, 147
 upwind, 147
 Numerical method, 145
 explicit, 145
 implicit, 145
 Numerical update, 161
 Euler, 151, 161, 173
 parallel, 230
 Runge-Kutta, 161
 sequential, 230
 Numerical update time, 175, 185

O

Objective function, 304, 418, 421
 unimodal, 307
 Obstruction, 108
 Occupancy, 15, 23, 158
 OCT. *See* Oscillating congested traffic
 Optimal speed. *See* Velocity
 Optimal Velocity Model. *See* Model
 Optimization problem
 constrained, 49
 Origin-destination matrix, 382, 418
 Oscillating congested traffic, 343, 349
 Oscillations. *See* Traffic wave
 Outflow, 70
 Overreaction, 257
 Overrun fuel cut-off, 387
 OVM. *See* Optimal Velocity Model

P

Parallel update. *See* Numerical update
 Parameter estimation, 96–97
 Parameter orthogonality, 312
 Parameter vector, 304
 Parsimony, 312
 Particulate matter, 379
 Passing rate, 274
 Paveri-Fontana model. *See* Model
 Payne's model. *See* Model
 Pedestrian, 92
 Pedestrian model. *See* Model
 Perception threshold, 220
 Perception time, 207

Phantom traffic jam, 258, 356, 360
 Phase. *See* Traffic phase
 Phase diagram, 340, 341
 boundary-induced, 351
 Phase velocity. *See* Velocity
 Pinch effect, 186
 Pinned localized cluster, 344, 349
 Platoon. *See* Vehicle platoon
 Platoon consistency, 317
 Plausibility conditions, 182
 PLC. *See* Pinned localized cluster
 PM. *See* Particulate matter
 Politeness factor, 244
 Pressure term. *See* Traffic pressure
 Priority road, 252
 Probability density, 437
 Probe vehicle, 368
 Psycho-physiological model. *See* Model
 Public transport, 404

Q

Quantity
 extensive, 69
 intensive, 69

R

Ramp flow, 71
 Ramp metering, 4, 404, 407
 capping strategy, 408
 Ramp term, 73
 Random walk, 136
 Randomness, 61
 Reaction distance, 179, 184
 Reaction time, 94, 127, 139, 173, 175,
 179, 185, 207, 257, 270
 effective, 208, 218
 Real-time estimation, 364
 Recuperation, 387, 390
 Regression, 304
 Relaxation term, 132
 Resignation effect, 219
 Response time, 207
 Responsiveness, 278
 Restabilization, 286, 295, 297, 344
 Right-overtaking ban, 243
 Ring road. *See* Closed system
 Road inhomogeneity. *See* Bottleneck
 Road-side unit, 413
 Roadworks, 406
 Robustness. *See* Model
 Root mean square, 330
 Route assignment, 3

Routing instability, 411
 Rule, 226, 228

S

Safe deceleration, 241
 Safe distance, 187
 Safe time gap, 158
 Safety, 406
 Safety criterion, 241, 242
 Safety distance, 158
 Safety time gap, 185
 Scale relation, 479
 SDD. *See* Stationary detector data
 Second-order model. *See* Model
 Section-based model. *See* Model
 Self-destructing prophecy, 411
 Self-organization, 344
 Self-regulation, 191
 Sensation time, 207
 Sensitivity
 parameter, 169
 Sensitivity analysis, 311
 Shock front, 84
 Shock wave, 84, 136
 propagation velocity, 87, 108
 Simulation, 3, 140, 294
 interactive, 245, 406
 software, 4
 Sink, 100, 108
 Slow-to-start rule, 232
 Social force. *See* Force
 Social-force model. *See* Model
 Source, 100, 108
 Source density, 71, 73, 74
 Source term, 137
 Space mean speed, 16, 68, 328
 Space-time diagram, 9
 Spatiotemporal diagram.
 See Space-time diagram
 Specific consumption, 392
 Speed
 adaptation time, 168, 175, 185, 287
 desired, 27, 30, 31, 94, 169, 181
 distribution, 27, 28
 effective, 68
 effective desired, 405
 free, 27, 303
 lane-averaged, 68
 local, 68
 synchronized, 28
 Speed adaptation time, 132
 Speed funnel, 406
 Speed limit, 405

S (cont.)

Speed synchronization, 375
 Speed variance, 16
 Speed-density diagram, 27, 82
 Spill over, 105
 SSE. *See* Sum of squared errors
 Stability. *See* Instability
 asymptotic, 261
 CFL. *See* Courant–Friedrichs–Lévy
 conditions
 Ljapunov, 261
 numerical, 140
 structural, 261
 Stability class, 295
 Stability diagram, 291, 339
 Standard deviation, 16
 Standard normal distribution, 143
 Statistical mode, 30
 Steady-state conditions, 130
 Steady-state equilibrium, 162, 170,
 194, 195
 cellular automata, 231
 Steady-state traffic, 118
 Stochastic process, 211
 Wiener, 212
 Stochastic variable, 210
 Stop-and-go mechanism, 258
 Stop-and-go traffic, 167
 Stop-and-go wave. *See* Traffic wave
 Stopping distance, 184, 251
 overall, 179
 Strategy matrix, 414
 String instability. *See* Instability
 Stylized facts, 361
 Sum of squared errors, 304
 absolute, 319
 mixed, 319
 relative, 319
 Supply, 55, 100
 Supply-demand method, 105, 149
 Synchronized traffic, 234, 345
 System
 closed, 108, 179, 294, 340
 extended, 266
 infinite, 339
 open, 264, 294

T

Taylor expansion, 154, 175, 276
 Taylor series. *See* Taylor expansion
 Telematics, 4, 404
 Test data, 303
 Three-phase theory, 233, 234, 345

Time gap, 14, 30, 94, 96, 185, 187
 desired, 34
 distribution, 30
 Time headway, 9, 30
 Time mean speed, 16, 328
 Time series, 25
 Time-to-collision, 211, 252
 Toy system, 294
 Traffic
 bicycle, 63
 congested, 88
 free, 88
 heterogeneous, 29, 62, 141, 164
 mixed, 63
 non-motorized, 63
 pedestrian, 63
 Traffic assignment, 404
 agent-based, 3
 Traffic breakdown, 25, 97, 165, 192,
 355, 403, 411
 Traffic demand, 340, 418
 Traffic density, 9, 17
 effective, 67
 Traffic dynamics
 hysteretic, 193, 262
 spatiotemporal, 40
 Traffic flow, 9, 15, 17
 microscopic, 15
 stationary, 434
 Traffic flow modeling, 55, 405
 Traffic instability. *See* Instability
 Traffic jam, 25, 96, 355
 Traffic light, 167, 168, 171, 178, 203, 250
 minimum duration of yellow phase, 473
 Traffic light control, 4
 Traffic phase, 340
 Traffic pressure, 134, 282
 Traffic state reconstruction, 40
 Traffic stream model. *See* Model
 Traffic wave, 10, 39, 127, 166, 231,
 257, 258, 343
 standing, 344, 349
 stationary, 76
 Trajectory, 7, 76, 167
 virtual, 371
 Trajectory data, 7
 Transport-diffusion equation, 122
 Transportation planning, 2, 55, 240, 404
 Travel time, 367
 expected, 367
 instantaneous, 373
 realized, 367
 total, 367, 368
 Triggered stop-and-go waves, 343, 349, 361

Trip distribution, [2](#)
 Trip generation, [2](#)
 Truck overtaking ban, [416](#)
 TSG. *See* Triggered stop-and-go waves
 TTC. *See* Time-to-collision

U

Update time. *See* Numerical update time
 Upwind. *See* Numerical integration
 Upwind finite differences, [148](#)
 User equilibrium, [19](#)
 Utility, [241](#), [414](#), [418](#)
 maximization, [241](#)
 Utility function, [240](#)

V

Validation, [43](#), [333](#)
 cross, [334](#)
 holdout, [333](#)
 inverse cross, [334](#)
 Variability
 inter-driver, [62](#), [313](#)
 intra-driver, [62](#), [313](#)
 Variable
 endogenous, [2](#), [383](#)
 exogenous, [2](#), [61](#), [205](#)
 Variable message sign, [4](#), [29](#), [411](#)
 Variance, [16](#)
 Variation coefficient, [16](#), [142](#), [210](#)
 Vasaloppet, [64](#)
 Vehicle kilometers travelled, [380](#)
 Vehicle length, [13](#), [215](#)

 average, [23](#), [31](#)
 effective, [93](#), [228](#)
 Vehicle platoon, [168](#), [196](#), [257](#), [359](#)
 Vehicle-driver unit. *See* Driver-Vehicle Unit
 Vehicular dynamics, [3](#)
 Velocity
 optimal, [168](#)
 phase, [291](#)
 propagation, [41](#), [231](#)
 stop-and-go wave, [41](#)
 Virtual vehicle, [168](#), [171](#), [203](#)
 Viscosity, [136](#)
 VKT. *See* Vehicle kilometers travelled, [380](#)
 VMS. *See* Variable message sign, [411](#)
 Von-Neumann conditions.
 See Boundary conditions

W

Wardrop's equation, [19](#)
 Wardrop's equilibrium, [19](#)
 Wave number, [273](#), [280](#)
 Weakest link, [356](#), [360](#)
 Wiedemann Model. *See* Model
 Wiener process. *See* Stochastic process

X

xFCD. *See* Extended floating-car data

Z

Zipper merging, [240](#), [417](#)